Performance Characterization and Energy Savings Assessment of a Radial Flux Surface Permanent Magnet Motor Technology

Alex Bulk and Omkar Ghatpande

National Renewable Energy Laboratory

NREL is a national laboratory of the U.S. Department of Energy
Office of Energy Efficiency & Renewable Energy
Operated by the Alliance for Sustainable Energy, LLC

This report is available at no cost from the National Renewable Energy Laboratory (NREL) at www.nrel.gov/publications.

Contract No. DE-AC36-08GO28308

Technical Report
NREL/TP-5500-85342
April 2023

Performance Characterization and Energy Savings Assessment of a Radial Flux Surface Permanent Magnet Motor Technology

Alex Bulk and Omkar Ghatpande

National Renewable Energy Laboratory

Suggested Citation
Bulk, Alex and Omkar Ghatpande. 2023. *Performance Characterization and Energy Savings Assessment of a Radial Flux Surface Permanent Magnet Motor Technology*. Golden, CO: National Renewable Energy Laboratory. NREL/TP-5500-85342. https://www.nrel.gov/docs/fy23osti/85342.pdf.

NREL is a national laboratory of the U.S. Department of Energy
Office of Energy Efficiency & Renewable Energy
Operated by the Alliance for Sustainable Energy, LLC

This report is available at no cost from the National Renewable Energy Laboratory (NREL) at www.nrel.gov/publications.

Contract No. DE-AC36-08GO28308

Technical Report
NREL/TP-5500-85342
April 2023

National Renewable Energy Laboratory
15013 Denver West Parkway
Golden, CO 80401
303-275-3000 • www.nrel.gov

NOTICE

This work was authored by the National Renewable Energy Laboratory, operated by Alliance for Sustainable Energy, LLC, for the U.S. Department of Energy (DOE) under Contract No. DE-AC36-08GO28308. Funding provided by the U.S. Department of Energy Office of Technology Transitions. The views expressed herein do not necessarily represent the views of the DOE or the U.S. Government.

This report is available at no cost from the National Renewable Energy Laboratory (NREL) at www.nrel.gov/publications.

U.S. Department of Energy (DOE) reports produced after 1991 and a growing number of pre-1991 documents are available free via www.OSTI.gov.

Cover Photos by Dennis Schroeder: (clockwise, left to right) NREL 51934, NREL 45897, NREL 42160, NREL 45891, NREL 48097, NREL 46526.

NREL prints on paper that contains recycled content.

Acknowledgments

The authors would like to thank ZEUS Motor Inc. for supporting this research by providing their technology and laboratory facilities to conduct this evaluation. The National Renewable Energy Laboratory (NREL) would like to specifically thank Tom Hopkins, Felipe Castillo, and Patrick Stoever for helping to conduct the experimental evaluation, troubleshoot lab setup issues, and develop analytical solutions for data post-processing. This report was prepared by NREL's Building Technologies and Science Center.

The authors would also like to express their gratitude to representatives of the North Carolina Advanced Energy Corporation and Yokogawa Electric Corporation for their assistance in setting up and troubleshooting the dynamometer lab bench. From NREL, the authors would like to thank Monali Mujumdar for managing the project and J.A. Colantonio for setting up the initial scope-of-work contracts and getting the project off the ground. Finally, the authors would like to thank Tom Hopkins of ZEUS and Venkatesh Chinde of NREL for their in-depth report review.

For more information, contact:
Alex Bulk
National Renewable Energy Laboratory
Email: alexander.bulk@nrel.gov

List of Acronyms

ΔkWh	delta (difference) of kilowatt-hours
AC	alternating current
ANSI	American National Standards Institute
ASHRAE	American Society of Heating, Refrigerating, and Air-Conditioning Engineers
DC	direct current
DOE	U.S. Department of Energy
HP	horsepower
HRSRM	high rotor pole switched-reluctance motor
Hz	hertz
kg	kilogram
kW	kilowatt
kWh/day	kilowatt-hours per day (a unit of measurement of energy consumed over one 24-hour period)
MHz	megahertz (a unit of electrical frequency; equal to one million hertz)
m/s	meters per second (a unit of measurement of velocity)
NCAP	NREL's Commercial Technology Assistance Program
NEMA	National Electrical Manufacturers' Association
NREL	National Renewable Energy Laboratory
Ph	phase
PMAC	permanent magnet alternating current motor
RF-sPMAC	radial flux, surface permanent magnet alternating current motor
RPM	revolutions per minute
SRM	switched-reluctance motor
V	volts
VFD	variable-frequency drive

Executive Summary

This project is part of the National Renewable Energy Laboratory's (NREL's) Commercialization Assistance Program to provide technical expertise to help emerging companies overcome technical barriers to commercialization. In this study, NREL has evaluated the efficiency and energy savings potential of a novel motor technology designed by ZEUS Motor Inc. located in Wheat Ridge, Colorado. The motor expands on the design of permanent magnet AC motors (PMACs) to create a new "radial flux, surface PMAC" (RF-sPMAC) motor. This new RF-sPMAC design is expected to outperform other novel motor technologies on the market. Here, the motor showed considerable energy benefits over typical induction motors. The motor benefits from a tightly packed magnetic steel and copper stator that allows the motor size to be reduced to a thin disc with an internal cavity $1/30^{th}$ the size of a traditional induction motor. The housing is also aluminum, which is magnetically benign. This eliminates the need for external cooling (up to motors sized to 25 HP), in addition to reducing power consumption.

The objective of this project is to compare the performance of the motor to that of an equivalent common alternative, and then model energy savings in two scenarios using those results. The project is therefore composed of two phases:

1. Laboratory characterization of the ZEUS RF-sPMAC under various torque and speed scenarios using a variable-frequency drive (VFD) to generate a complete performance map and compare with available data on an induction motor with equivalent electrical and mechanical specifications.
2. Modeling estimate of the daily and annual energy savings and demand reduction when comparing to those of an equivalent induction motor when used in (1) a conveyor belt system and (2) a water pump system.

In phase 1, the 15 HP high-efficiency RF-sPMAC motor and drive were observed to perform with considerably higher efficiency than the baseline at every torque load and speed setpoint. The IE2-rated baseline was especially outperformed at lower torques and reduced speeds in which the RF-sPMAC motor consumed up to 34.2% less power. The maximum difference in efficiency was 28.4% (85.5% by the RF-sPMAC, 57.1% by the baseline), which occurred at 1,200 RPM and at the lowest torque load setpoint (14.7 Nm). The ZEUS RF-sPMAC motor exhibits the optimum benefit under these conditions due to the fact that losses in efficiency were minimal as torque was reduced. This trend was contrasted by the baseline motor, which exhibited significant loss with respect to torque. At the highest torque load (64.9 Nm) and rated speed (1,800 RPM), the ZEUS RF-sPMAC motor and drive reached a maximum efficiency of 92.3%, whereas the baseline motor was 87.4% efficient. This 92.3% efficiency was significant for a 15 HP motor with these specified ratings when coupled with VFD-induced losses.

The performance characterization used a lab bench located at ZEUS's facilities that was overseen and approved by NREL to ensure accurate calibration of sensors and procedural compliance with standards. The performance characterization was conducted in close accordance with the ANSI/ASHRAE standard 222-2018 method of test for electrical power drive systems [1], and following the procedures of the North Carolina Advanced Energy Corporation, an ISO 17025-accredited laboratory for characterizing motor performance. To evaluate efficiency improvements against a baseline, an induction motor with comparable specifications was

selected from the U.S. Department of Energy's (DOE's) *MotorMaster-Plus* database of 16,359 motors [2].

In phase 2, the ZEUS motor system realized very significant energy and operating cost savings compared to conventional induction motor systems. Realistic conveyor and pump system parameters were selected that would yield an appropriately sized application for the 15 HP RF-sPMAC and matching baseline. These systems were chosen because the global conveyor market in 2018 was $4.2 billion per year, growing to an estimated $5.48 billion in 2026 [3], and pumps in commercial buildings use up to 18% of what consumes 35% of total U.S. electricity [4, 5]. The conveyor energy consumption was modeled using an engineering calculation tool that was developed based on the equations for calculating the operating power of "belt conveyors with carrying idlers," ANSI/ISO standard 5048-1989 [6, 7]. Conveyor structural and operational parameters were adjusted to assess energy savings under four scenarios: (A) high speed/high torque, (B) high speed/low torque, (C) low speed/high torque, and (D) low speed/low torque. Energy savings from each scenario were calculated at (A) 28.5 kWh/day, 10.4 MWh/year (9.20%); (B) 28.2 kWh/day, 10.3 MWh/year (26.5%); (C) 3.54 kWh/day, 1.29 MWh/year (14.9%); and (D) 1.34 kWh/day, 0.488 MWh/year (10.2%). As torque was reduced in the conveyor, the percent savings increased. The baseline energy, however, was significantly reduced under these scenarios, diminishing the magnitude of savings.

With a 16¢/kWh utility rate, cost savings would range between $1,664.31 yearly savings under high speed/high torque conditions, but would be diminished to $78.03 yearly savings under low speed/low torque conditions. These savings are for an individual conveyor section: Typically, operations require numerous conveyor sections, and so these savings would compound based on the number of individual motors replaced. The energy consumption per ton*mile was calculated as high as 0.36 Wh/ton*mile under the high-speed/high-torque scenario down to 0.017 Wh/ton*mile under the particular parameters analyzed.

The pump system power was modeled from a set of derived hydraulic equations that estimate the speed and torque enacted on the pump motor from flowrates and pressure heads that the motor might have to provide in a common commercial pump system. A set of pump parameters along with a yearly load profile were assumed for this study. Energy savings from two load profile scenarios were evaluated—(A) "even" distribution and (B) "uneven" distribution—because no pump parameters individually affected speed and torque similarly to the conveyor analysis. The "even" distribution scenario resulted in 10.9 ΔkWh/day and 3.97 ΔMWh/year of energy savings, or 15.6%, whereas the "uneven" distribution scenario resulted in 11.1 ΔkWh/day and 4.00 ΔMWh/year of energy savings, or 16.3%. At a 16¢/kWh utility rate, cost savings were calculated in the range of $635–$651 across scenarios. This savings number is highly dependent on individual pump-motor setup and its corresponding yearly load profile.

Table of Contents

List of Tables

List of Figures

1 Introduction: Project Description and Technology

The purpose of this project is to (1) evaluate the performance of a radial flux, surface permanent magnet AC (RF-sPMAC) motor and VFD experimentally and compare its efficiency to an equivalently rated induction motor, and (2) estimate the energy savings potential from retrofitting an RF-sPMAC motor to an appropriately sized conveyor and pump application under different speed and torque scenarios.

The experimental assessment to characterize motor and VFD performance was conducted in close accordance with ANSI/ASHRAE standard 222-2018 [1]. Additional procedures conducted beyond these guidelines were followed according to regular procedures conducted to evaluate motor and drive system performance by the ISO 17025-accredited, North Carolina Advanced Energy Corporation. Advanced Energy provided feedback and assistance for conducting these procedures in this study by coordinating closely with engineers on-site. To conduct the evaluation, ZEUS engineers purchased and configured the dynamometer test bed based on recommendations from Advanced Energy and Yokogawa Electric Corp. (power analyzer manufacturer). Then, NREL reviewed and approved all calibration certificates and initial electrical data to ensure standard compliance prior to monitoring experiments at ZEUS's facility.

The performance characterization involved mapping the torque, speed, input/output power, and efficiency of each motor/drive using a dynamometer, torque/speed transducer, and power analyzer. A dynamometer is a device that supplies a controlled braking torque to the motor. When using a VFD to adjust the motor speed, this allows the motor and drive system to be controlled to various torque and speed setpoints such that the input (from the power analyzer) and output power (from the torque/speed transducer) can be "characterized" at each of these setpoints. If enough setpoints are evaluated across the motor's operating range (rated RPM and full-load torque), the complete performance of the motor and drive system can be "mapped," as done in this study. The performance was then compared to a common induction motor with an equal rated RPM, full-load torque, HP, voltage, and current selected from the U.S. Department of Energy's (DOE's) *MotorMaster-Plus* tool [2].

Predicted energy savings was modeled in an appropriately sized conveyor and pump system. This was done by using various modeling tools to calculate certain torque and speed scenarios that can be imposed on the motor and drive system (high speed/high torque, high speed/low torque, low speed/high torque, low speed/low torque). The calculated torques and speeds were interpolated to the performance maps of the RF-sPMAC and baseline motors to calculate predicted demand. Expected system operation was then used to integrate demand over time to predict energy savings. To predict energy savings in a conveyor system, NREL had previously developed a modeling tool to streamline these calculations [7]. The framework of the tool is based on ANSI/ISO standard 5048-1989 for calculating the operating power and tensile forces in straight belt conveyors [6], and therefore will be used to calculate energy savings in this study. To predict power savings in a pump system, a modeling tool was used to calculate certain torque and speed scenarios by varying fluid flowrates and pressure heads that yielded reasonable motor demand. The energy savings depends on the operating conditions of the motor throughout the year—two scenarios with even and uneven hourly distribution for these conditions were used for analyzing energy savings.

1.1 Technology Description

ZEUS Motor Inc. has designed a novel radial flux, surface permanent magnet AC motor that is suitable for the most common range of startup torque-speed applications designated with a NEMA-B (National Electrical Manufacturers' Association) rating. Unlike a standard induction motor, which uses a rotor with metal bars wound in an electrically conductive coil like the stator, a permanent magnet AC motor has rotor poles composed of permanent magnets. To understand what benefits are induced by this difference in design, first we must go over the operation of an AC induction motor:

An AC induction motor generates a magnetic field that rotates around the motor when a 3-phase AC current is fed through the stator [8, 9]. The speed of the magnetic field is the synchronous speed, which is double the ratio of frequency to the number of magnetic poles [8]. Induction from the magnetic field causes current to be generated through the rotor windings, which induces its own magnetic field that opposes the stator's magnetic field. Lenz's law then causes the rotor to spin, because it will try to "catch up" to the motion of the magnetic field in the stator [9]. The "slip," or difference between the synchronous and rotor speeds, defines the torque [10]. To handle higher torques, the rotating magnetic field must compensate for increased slip as the rotor speed is reduced by feeding more current [11].

Unlike an induction motor, a PMAC motor uses a rotor with permanent magnets rather than conductive windings. Therefore, the magnetic field in the rotor that is opposing the magnetic field in the stator windings is not generated by a current and instead by the magnetic material used. Lacking the need to generate current in the stator reduces losses in the rotor, which results in improved efficiency. Depending on the magnetic material used, the lifetime of the motor can also be extended compared to an induction motor [12]. PMAC motors are classified based on two criteria: First, whether they are surface or interior PMAC motors, meaning that the magnets are either mounted to the surface of the rotor, or within the inside of the rotor [13]. The motor used here designed by ZEUS is a surface permanent magnet design. Typically, the surface PMAC motors suffer from lower torque density compared to interior PMACs, but benefit from reduced torque ripple when coupled with a variable-frequency drive, or VFD [13]. The use of a VFD with a PMAC motor is necessary for optimal performance in addition to operating at reduced speeds [14].

Both PMACs and induction motors can only operate at a single speed depending on the AC current frequency. Therefore, a VFD controls speed by controlling the input AC frequency to the motor. This is done by first using a rectifier and filter capacitors to convert AC voltage to DC [15]. Power transistors then use pulse-width modulation to change the DC voltage while switching on and off rapidly in order to generate a new AC "sinusoidal" waveform [7, 15]. The frequency that the voltage is switched, or the "carrier frequency," is extremely high and so changing transistor states at this frequency induces losses that lower system efficiency depending on the extent to which speed is reduced [7]. This carrier frequency also causes the current to "ripple," which induces a downstream torque ripple effect. The current ripple also of course generates a ripple in the magnetic field, which results in losses in the overall motor/drive system. A benefit of PMAC motors is that these losses are reduced compared to an induction motor in which its rotor magnetic field is generated by an induced current from the stator [14]. Certain

configurations of PMAC motors, such as the one evaluated here, also don't require position feedback, which reduces the demand by the VFD and contributes to overall efficiency [12, 14].

As efforts to increase the efficiency of induction motors have stalled, PMAC motors have received more attention over the past few decades since improvements have yielded greater efficiencies [14, 16-18]. In 2014, an axial flux rotor structure was proposed that would yield the highest peak efficiencies observed [17]. PMAC motors can be classified as axial flux, or radial flux, depending on how the magnet poles are oriented with respect to the stator coils [13]. Previously, ZEUS had developed a radial flux, surface PMAC (RF-sPMAC) motor rated 15 HP and 1,800 RPM that outperformed any previous PMAC motor by using a novel 12-pole, 18-slot, concentrated coil, fractional-slot design described in Ref. [14]. The performance of that model was verified by Advanced Energy [19], who determined the efficiencies to be higher than NEMA "super-premium efficiency"-designated, or EIEC IE5 classifications by over 3% [14]. The motor evaluated in this study is a matured prototype called "Series 225": an upgraded version of that motor with a proprietary design. The new model's efficiency is partially attributed to its air-cooling system and use of less material [20], which is the result of 15 iterations to optimize the motor's design. The design was not constrained to make its frame identical, physically, to a standard NEMA induction motor frame with the same power output. The motor is only 13" in diameter and 2.25" in active axial length (where the rotor's permanent magnets face against the stator's electromagnets), which is around 1/3 of the weight and a quarter of the volume of common induction models. The manufacturer also touts an extended lifespan due to interior encapsulation and demagnetization protection [20].

A catalogue photo of the evaluated 15 HP Series 225 model ZEUS RF-sPMAC motor model is shown in Figure 1. Motor specifications are provided in Table 1. Table 1 below shows the ZEUS Motor's "S1" duty rating, at which it can be run continuously for an unlimited period.

Figure 1. Catalogue photo of the evaluated 15 HP RF-sPMAC motor

Figure courtesy of ZEUS Inc.

Table 1. RF-sPMAC ZEUS Motor Specifications

Motor Model #:	Series 225
Motor Output Rating:	15 HP
Motor Voltage (V):	480 VDC
Motor Rated Current (A):	22.3 A
Motor Rated Speed (RPM):	1,800
Motor Frequency (Hz):	180 Hz
Full-Load Torque:	59 Nm
Motor Weight:	125 lbs
Motor Duty:	S1

The evaluated RF-sPMAC was fully characterized at reduced speeds using a VFD. In the lab, a Yaskawa A1000 VFD was used to evaluate the RF-sPMAC. Due to its unique design and rotor magnet configuration, ZEUS does not use default VFD settings and has instead developed a unique VFD control scheme to operate their motor most efficiently. However, during the evaluation, issues with the electrical instrumentation to the VFD inputs were encountered. Therefore, drive efficiency data from a previous Advanced Energy evaluation of the ZEUS motor was instead used to characterize the motor and drive system [19]. The VFD used in that evaluation was an Allen Bradley Powerflex 755 model. That VFD was configured accordingly to effectively operate the unique RF-sPMAC, but the Yaskawa VFD has been determined to optimize the overall system performance of the ZEUS motor and drive more effectively than the Allen Bradley. This study is focused on improvements in the motor design and therefore this does not inhibit the evaluation.

1.1.1 Baseline Motor

The baseline motor and VFD were selected from the U.S. Department of Energy (DOE)'s MotorMaster+ database [2]. A standard induction motor rated at the same horsepower, rated speed, input voltage, full-load torque, and closest electrical specifications was used for the evaluation that has an IE2 efficiency rating. The database only contains manufacturer data; therefore, it should be noted that it may not be indicative of the actual performance of the model from third-party performance testing. To protect the manufacturer, this motor will only be referred to as the baseline in this report.

Motor and drive system efficiency with a VFD was estimated using "idealized VFD efficiency factors" theorized by Wallbom-Carlson to account for losses from the VFD and losses generated in the motor by the VFD [21, 22]. These efficiencies were calculated within the NREL conveyor modeling tool's interface containing the MotorMaster+ data and have been verified with performance data from other baseline induction motors in the lab [7]. Idealized VFD efficiency factors were interpolated using 2D fourth-order regression fit to the speed and torque data.

1.2 Modeling Parameters and Conditions

The performance of the novel energy-efficient RF-sPMAC motor designed by ZEUS was compared to the selected baseline in a realistic conveyor and pump application to assess potential energy savings. Parameters in these modeling applications were configured such that four unique speed/torque scenarios could be assessed. These parameters were selected from listed references due to yielding an "appropriate fit" for the specifications for both the RF-sPMAC and baseline motors. A list of the selected parameters and rationale behind their selection is provided in the following sections, along with a description of the modeling procedure.

1.2.1 Conveyor Energy Model

The energy of the evaluated motor and drive systems when coupled with a conveyor was determined by using a modeling tool with realistic conveyor parameters that would generate reasonable speeds and torques within the motors' operating range. Overall, this was done by calculating the speed and torque that a conveyor would demand from the motor and drive and then integrating across the conveyor operation time. The speed and torque were input to a 2D, fourth-order regression surface fit to the characterized performance data from each motor to calculate the efficiency and power consumption. To calculate the motor speed required by a conveyor, one only needs to know the belt speed and driving roller diameter (the roller mounted to the motor shaft). Calculating the torque is however more complex, and requires an extensive list of parameters that are used in the equations listed in the ISO 5048 standard for belt conveyors with carrying idlers [6]. NREL has developed a "conveyor energy calculator tool" for related research that utilizes this standard in a streamlined interface that allows a user to enter a set of conveyor parameters and motor performance data in order to calculate the energy savings. The overall procedure used by the tool is outlined in Figure 2. This tool will therefore be used here in this study.

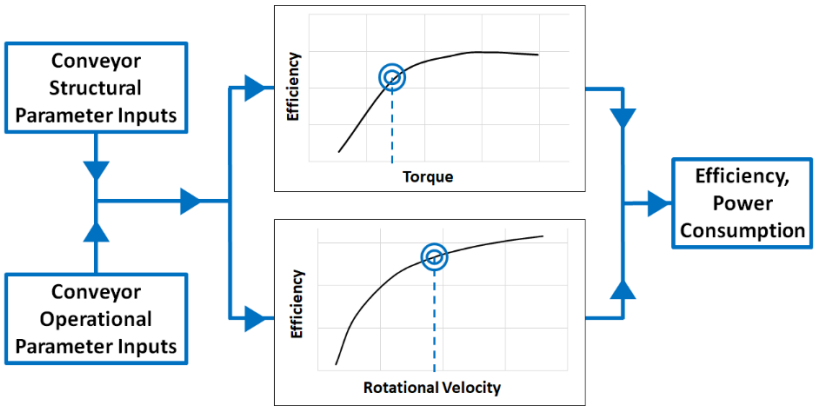

Figure 2. Conveyor energy calculation tool—general procedure [7]

Structural parameters are associated with the physical structure of the belt that do not change throughout daily industrial operations (e.g., belt and idler mass, section width). Operational parameters can change throughout daily operation, (e.g., belt speed, conveyed product material densities), or dictate operation (the daily/weekly operation schedule). Because structural and operational differences between conveyors affect the speed and torque demand on the motor, energy consumption will vary widely between any two conveyors using the same motor/drive system. Although here, realistic parameters will be selected that yield demand on the motor that

is an appropriate fit for the motors' size (near its rated speed and full-load torque), some of these parameters will therefore be altered to assess energy savings at high speed/low torque, low speed/low torque, and low speed high torque applications.

A 15 HP motor was found to be an appropriate fit for a generic mining application. Mines typically use conveyors to remove excavated material from the interior of the mine to an external processing location. An internet search for common mining conveyors used with a 15 HP motor generated the list of structural parameters shown in Table 2 below. The values for the parameters found through the search were input to the conveyor tool and then adjusted until the speed and torque approached the rated torque and speed of the motor. Table 2 shows these final parameter values that were used for every speed/torque scenario. Note that bituminous coal was used as the example material here, yet the material is not critical with respect to the overall torque since conveyor installations used to transport other materials would adjust other parameters to account for changes in material density.

Table 2. List of Structural Conveyor Parameters Used in Conveyor Energy Model

Parameter	Value
Section length	80 ft
Incline angle	15°
Number/width of idler rollers	3x 1 ft-wide
Idler roller: inner/outer diameter of rotating part	2.5"/6"
Idler material	Stainless steel
Belt width/thickness	3 ft / 1.4 cm
Belt material	Silicone rubber
Drive roller diameter	4"
Material density	50 lb/ft^3 (Bituminous coal as example material)
Guide friction coefficient	0.03 (kinetic between coal and stainless steel [23])

An image of the type of three-roller trough-style mining conveyor that is modeled using the above parameters is shown in Figure 3.

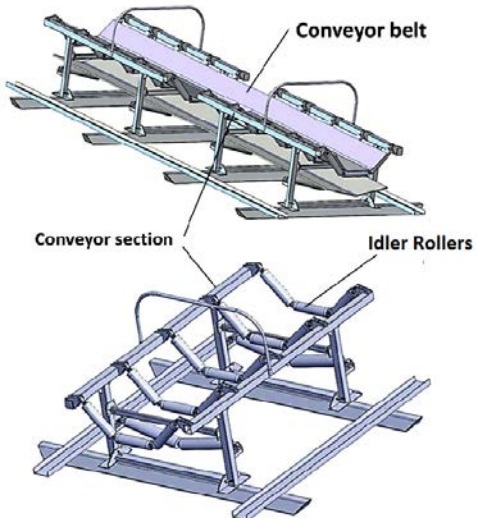

Figure 3. Shape of three-idler trough-style conveyor used for energy savings estimate

Image modified from Ref. [24]

The feed rate of material onto the belt used an example 24-hour shift scaled to the average tons of coal produced per miner-hour in the United States [25], assuming one conveyor section (i.e., one conveyor motor) was used per miner. Here, a "miner" refers to a machine that excavates coal and feeds it onto a conveyor. The average production was scaled across a production day, which was scheduled with a 10-hour day shift, and two 8-hour evening and night shifts with two crossover periods. Output is reduced 75% during the evening shift and 50% during crossovers and lunches (per shift). This schedule was selected based on a typical mine schedule and is not specific to any real conveyor but was used to estimate changes in torque throughout an operation day. The feed rate at each hour of the day used in the energy savings calculation is shown in Table 3.

Table 3. Conveyor Feed Rate Operation Schedule Used in Evaluation

Hour Range	Feed Rate (tons/hr)	Hour Range	Feed Rate (tons/hr)
6:00 AM – 7:00 AM	4.24	8:00 PM – 10:00 PM	8.48
7:00 AM – 12:00 PM	8.48	10:00 PM – 11:00 PM	4.24
12:00 PM – 1:00 PM	4.24	11:00 PM – 2:00 AM	6.36
1:00 PM – 3:00 PM	8.48	2:00 AM – 3:00 AM	3.18
3:00 PM – 4:00 PM	6.36	3:00 AM – 5:00 AM	6.36
4:00 PM – 7:00 PM	8.48	5:00 AM – 6:00 AM	3.18
7:00 PM – 8:00 PM	4.24		

To keep the analysis as realistic as possible, only a single parameter was altered to assess energy savings under low torque applications. To avoid drastically altering the value of this parameter beyond what would constitute a realistic configuration, the structural parameter that has the greatest effect on torque was selected. Previous studies have determined the spacing of the idler rollers on the conveyor to be the most influential parameter [7], therefore high torque and low torque scenarios used a 0.8 meter (typical), and 8 meter (atypical) spacing, respectively. Likewise, the rotational speed was altered between high speed and low speed scenarios by simply adjusting the belt speed between 30 ft/s and 2 ft/s, respectively, both of which could be

common belt speeds in different mining applications [26]. Unfortunately, belt speed is used in equations for calculating torque under the ISO 5048 standard calculations [6], therefore the same torque cannot be assessed under the high speed/high torque and low speed/high torque scenarios. The procedure for applying these calculations is discussed in Section 2.2. When adjusting belt speed while feed rate was held constant, here we assumed that the material on the conveyor could stack infinitely high without spilling over the belt.

1.2.2 Pump Energy Model

The energy of the evaluated motor and drive systems when coupled with a pump was determined by using a modeling tool with variable fluid flowrates and pressures that yield reasonable motor demand. Overall, this was achieved by changing the motor speed driving the pump and the pressure head in the hydraulic system. As in the previous conveyor model, the speed and torque were input to a 2D, fourth-order regression surface fit to the characterized performance data from each motor to calculate the motor efficiency and power consumption.

A 15 HP motor is commonly used to drive pumps installed in commercial buildings for applications like chilled water loops, hot water supplies, condensers, pressurized water sprinkler systems, grey water, and potable water supply systems. Depending on the application, some of these pump systems include a variable-frequency drive (VFD) to control the flow rate of the pump, resulting in energy saving compared to mechanical throttling of valves. However, some pumps are still operated without VFDs to maintain pressure in a closed loop system within a required range.

Table 4 lists the rated pump parameter assumptions compatible with a 15HP motor. The pump fluid was assumed to be water with its density as 1,000 kg/m^3. Pump model parameters were assumed based on common models used in a typical commercial building. These parameters included a rated flow rate of 502gpm, 25m of rated pressure head, and a 70% pump efficiency. Pump parameters were used as inputs to the pump model equations described in Section 2.3.

Table 4. List of Pump Parameters Assumptions Used in Pump Energy Model

Parameter	Value
Rated Pump Flow	114 m^3/h (502 gpm)
Rated Pump Pressure Head	25 m (82 ft/35.5 psi)
Pump efficiency	70%
Fluid	Water
Fluid density	1,000 kg/m^3

For this analysis, we considered the yearly working hours using a 12-hour workday, 5 days per week, and 52 weeks per year for a total of 3,120 hours out of 8,760 possible yearly hours. Because flowrate and pressure affect torque and speed, only two scenarios were assumed for the study, unlike the four used in the conveyor model: (1) even distribution and (2) uneven distribution. The even distribution divided the 3,120 yearly hours equally in between various pump demand conditions with 156 hours per operating point. The uneven distribution varied the 3,120 yearly hours irregularly between different operating points. Figure 4 shows the pump demand hours for each condition in the two scenarios considered.

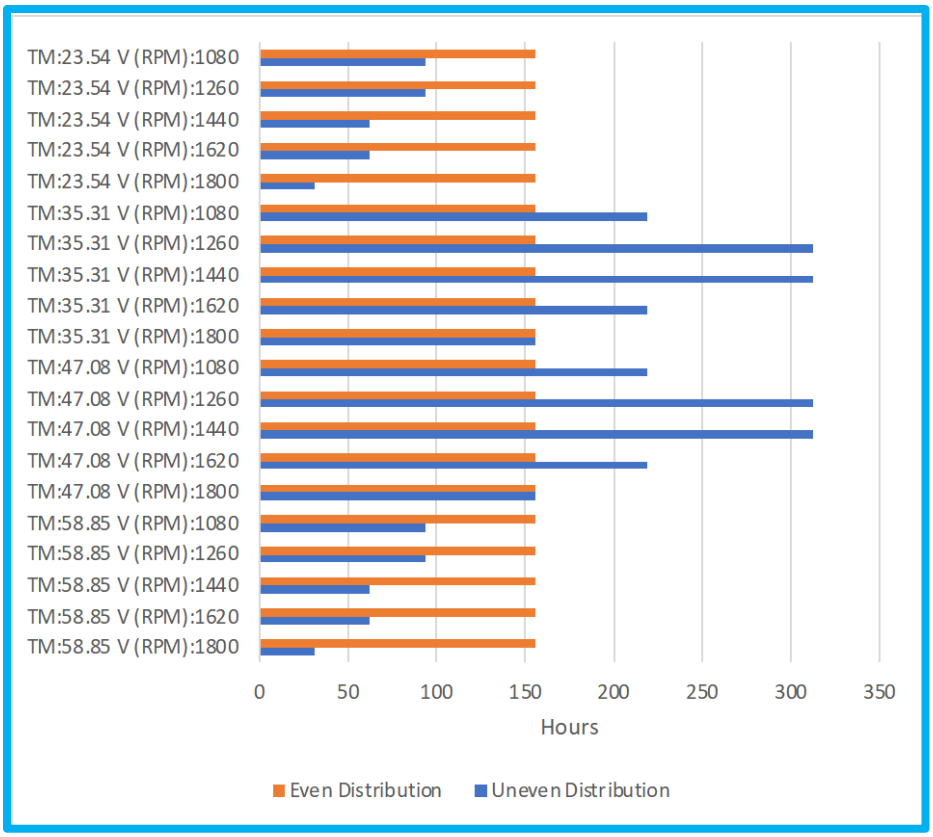

Figure 4. Load profile for motor shaft power at various torque (TM) and shaft speeds (V)

In the "uneven distribution" scenario, the flowrate and head pressure parameters fluctuated across their operating range to obtain the required motor shaft power. The flow rate through the pump ranged from between 60 and 100% of the rated flow rate at increments of 10%. The pressure head ranged between 40 and 100% of the rated head pressure at increments of 20%. Motor output parameters like torque (T_M) and shaft speed (V) were calculated from these different pump operating conditions as indicated on the Y-axis of Figure 4.

2 Experimental and Modeling Procedures

This section provides details pertaining to the experimental setup and procedure for the motor/drive performance characterization, as well as the procedure for analyzing the energy consumption of the RF-sPMAC motor when retrofit to a standard induction motor in an example conveyor and pump scenario. The performance characterization assessment was guided by and references practices published in ANSI/ASHRAE standard 222-2018 Section 7 [1], as well as regular practices of ISO 17025-accredited, Advanced Energy Corp. NREL is not a rating entity; however, the test procedure and guidelines for measurement outlined in this standard were closely followed where applicable. The motor performance characterization was conducted at ZEUS's facilities in Wheat Ridge, CO, and ZEUS supplied all measurement equipment. NREL monitored the evaluation and approved equipment/validated calibration certificates to ensure adherence to the standard guidelines and that measurement uncertainty fell within the range specified by the standard. One error in the measurement data was found with the inverter input electrical measurements, and therefore inverter efficiencies were not collected from this performance characterization. Instead, inverter data was acquired from a VFD used in a dynamometer evaluation conducted on the earlier model of the 15 HP ZEUS motor by Advanced Energy in Ref. [19] as described in the previous section.

The equations and modeling techniques used to estimate energy savings between the ZEUS RF-sPMAC motor and the baseline induction motor are described in detail in Ref. [7] for the example conveyor system, however brief details of the procedure are described in Section 2.2. The equations and procedure used for estimating energy savings in the example pump system are described in detail in Section 2.3. Standard hydraulic equations were derived into the modeled pump equations for the purposes of this study.

2.1 Motor/Drive System Performance Characterization

The 15 HP RF-sPMAC motor was mounted to the dynamometer test bench shown in the Figure 5 test schematic while being controlled by the Yaskawa VFD. The dynamometer load motor was connected to a torque and speed transducer to measure the output power, and the RF-sPMAC was connected to a precision power analyzer to measure input electrical power. To ensure synchronization of data, the torque and speed transducers were also connected to the power analyzer. Again, the input power to the Yaskawa VFD was not collected due to unresolved errors in the measurements from the power analyzer.

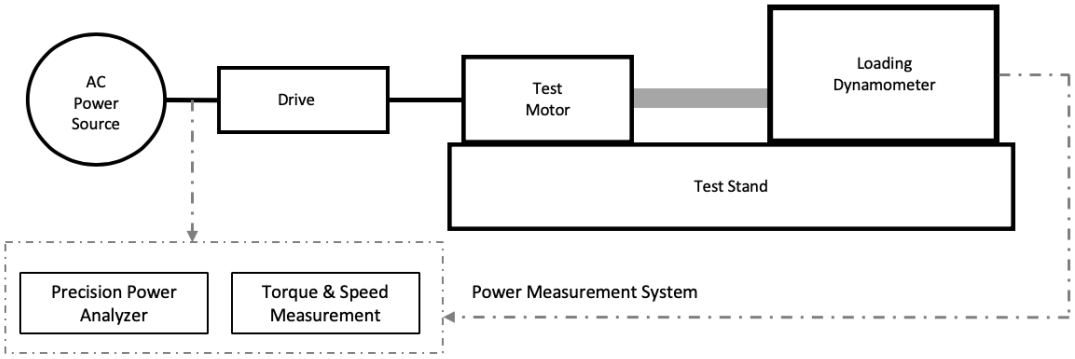

Figure 5. Schematic of dynamometer experimental setup

The range of speeds and torque setpoints that were measured are indicated in Table 5. The ZEUS motor is pre-fabricated with eight resistance temperature detectors (RTDs) at different motor coil locations throughout the motor circumference. Therefore, temperature measurements used these pre-fabricated RTDs. Prior to testing, the motor was thermally stabilized at 100% torque load at 1,800 RPM until there was less than 1°C temperature change in each of the RTDs over a 30-minute period. Following thermal stabilization, the torque was increased to 110% torque load at 60 Hz speed as the first measured setpoint. Then, the torque was reduced to the next torque setpoints while holding speed constant. Torque was then evaluated from the highest to lowest torque at the next lowest speed until all setpoints were measured. Each setpoint was stabilized for at least 10 seconds before recording data.

Table 5. List of Dynamometer Characterization Torque and Frequency Setpoints

Torque (%, Nm)	Motor Speed (Hz) 60	46.7	40	20	10
	Approximate Motor Speed (RPM) 1,800	1,400	1,200	600	300
110, 64.9	x	x	x	x	x
100, 59.0	x	x	x	x	x
90, 53.1	x	x	x	x	x
75, 44.3	x	x	x	x	x
50, 29.5	x	x	x	x	x
25, 14.8	x	x	x	x	x

An image of the RF-sPMAC motor mounted to the dynamometer test setup when conducting the performance characterization is shown in Figure 6. At each torque/speed setpoint listed above, the following data was recorded in accordance with ANSI/ASHRAE 222-2018 as an average across a 5-minute period (electrical measurements were recorded with respect to phase), the first six parameters of which will be reported here:

- Speed (RPM)
- Torque (N-m)
- Percent Full-Load Torque (%)
- System Efficiency (%)
- Input electrical power (W)
- Output electrical power (W)
- Current (A)
- Voltage (V)
- RTD Temperature (°C)
- Frequency (Hz)
- Total Voltage Harmonic Distortion (%)
- Total Current Harmonic Distortion (%)
- Voltage/Frequency Ratio

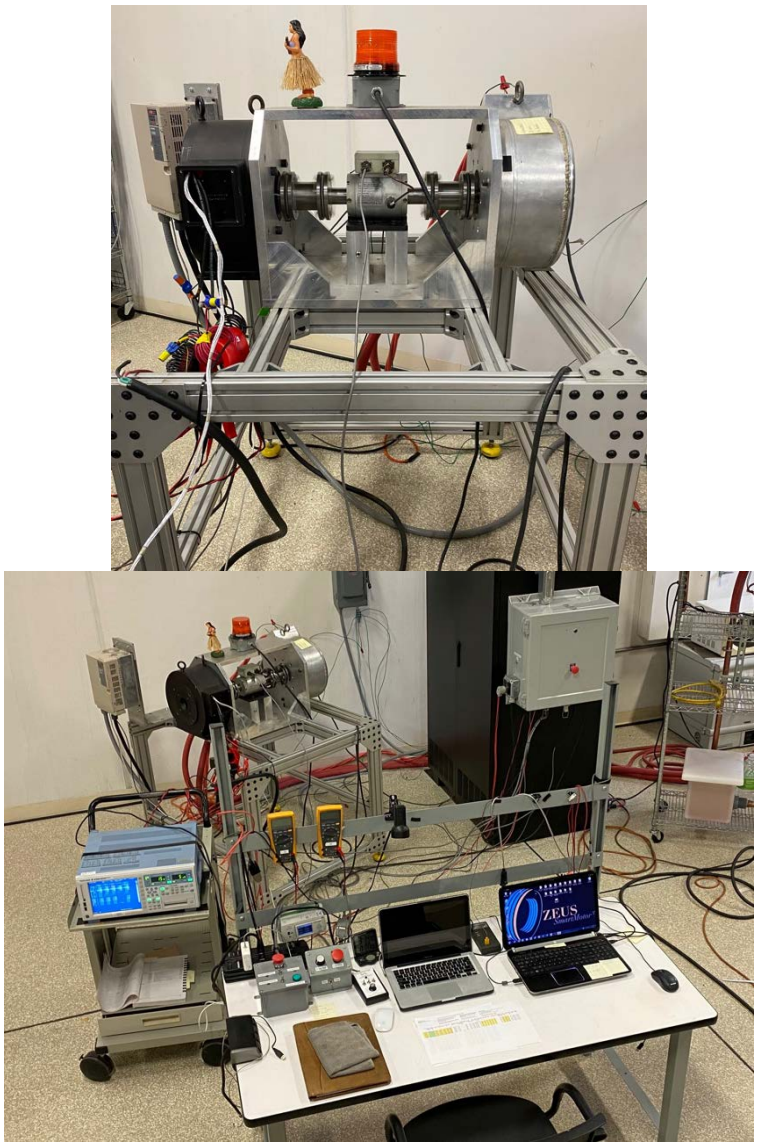

Figure 6. Images of ZEUS RF-sPMAC on dynamometer test bench at ZEUS facilities

Prior to conducting the evaluation, calibration certificates and initial measurement data were reviewed to ensure that their accuracy was within ANSI/ASHRAE 222 limits:

- Electrical measurements within ±0.2%
- Time measurements within ±0.5%
- Rotational velocity measurements within ±1 RPM
- Torque measurements within ±0.2%
- Temperature measurements within ±1.1°C/±2°F

The power analyzer had an update rate set to 500 ms for display capture and was used to capture both the input AC power and the output shaft power in order to calculate efficiency. The torque transducer was rated within twice the load torque, and the full-scale capacity of the dynamometer

was within double the rated power of the RF-sPMAC motor. Shielded cables were used to improve electrical noise immunity of the measured speed/torque signals.

The power source voltage supplied to the motor/drive was kept at the rated RMS (root mean squared) voltage and rated frequency within ±0.5% according to ANSI/ASHRAE 222. The max deviation of a particular RMS phase voltage from the average across all phases was checked and ensured to be less than ±1%. The power supply source impedance was within ±1%, and the total harmonic voltage distortion at no load was less than 3%. The cable length between the drive module and the motor was less than 20 feet.

The measurement equipment used for the laboratory evaluation is listed in Table 6. Each equipment item used was calibrated within the calendar year prior to the evaluation by recognized certified calibration testing entities. NREL and ZEUS have access to calibration certificates, which can be provided upon request. ZEUS used a custom AC dynamometer using a Siemens 1LE22212B B114AA3 model 15 HP motor to load the motor and a Yokogawa WT1806 precision power analyzer to record electrical measurements. A Himmelstein Ultra-Precise 48004P digital torquemeter was paired with the dynamometer that measured both speed and torque.

Table 6. Summary of Measurement Equipment Used To Conduct Motor/Drive Performance Characterization at ZEUS's Facilities in Wheat Ridge, CO

Measurement	Metric	Make	Model	Serial Number	Accuracy	Calibrated Prior to Test?
Power Out	Torque	Himmelstein	48004P	48004P07110112	±0.024%	Confirmed
Power Out	Speed	Himmelstein	48004P	48004P07110112	±0.08%	Confirmed
Power In	Voltage/ Current	Yokogawa	WT3000	N/A	±0.16%	Confirmed
Load Motor	N/A	Siemens	1LE22212B B114AA3	Q2-E16T4017GPE7	N/A	N/A

2.2 Conveyor Modeling Analysis Procedure

As stated, the calculations used in the NREL conveyor energy calculation tool were derived from equations used in ANSI/ISO standard 5048-1989 [6]. The tool is open-source upon request. More detailed background and rationale behind the equations used, and step-by-step instructions for using the tool are provided in Ref. [7]. The tool can be used for any straight belt-type conveyor.

The conveyor modeling tool is divided into six interface pages. Conveyor structural parameters are input on one user interface, a daily operation schedule is input on another, and baseline and proposed motor/drive performance data are entered on two additional interfaces. Operational parameters on the second page are entered separately for each unique operation "period" defined as a range of time that those parameters are constant. An output page shows the total daily kWh consumption for the motor/drive system(s) and ΔkWh savings between the baseline and proposed motor and drives. A final interface page is then used to enter a yearly operation schedule to calculate yearly consumption and/or savings.

The ISO 5048 standard states that the required torque is calculated based on the sum of internal frictional resistances along the conveyor section as described in equation 1:

$$T_M = \frac{d}{2}(F_H + F_N + F_{st} + F_S) \quad (1)$$

where d is the outer diameter of the driving roller (connected to the motor shaft), F_H is the "main resistance," F_N is the "secondary resistance," F_{st} is the "slope resistance," and F_S is the "special resistance." The main resistance, which is defined as the sum of resistances within the idlers, belts, and pulleys within the "carry-through region" of the belt (main region between loading and unloading), is calculated from Coulomb's friction law according to:

$$F_H = fLg\left[Q_R + 2Q_B + \frac{T(t)}{V(t)}\right]\cos(\delta) \quad (2)$$

where f is the "artificial friction factor," L is the section length, Q_R is the unit mass of the rotating parts of the idlers, Q_B is the unit mass of the belt, T(t) is the feed rate of material (conveyed product) onto the belt, V(t) is the belt speed, and δ is the belt incline angle (0° = horizontal). The unit masses are defined as mass per unit length of the conveyor section. Idler spacing therefore significantly affects the idler unit mass.

The secondary resistance is defined as the sum of the frictional resistances between the material and belt, and material and guide/skirt boards in the loading/unloading region. The equation used here was simplified from the ISO 5048 standard based on reasonable assumptions listed in [7]:

$$F_N = T(t)V(t) + \frac{T(t)^2}{\rho(t)b_t(t)^2} \quad (3)$$

where ρ(t) is the material density and $b_1(t)$ is the width of the conveyor section (with respect to time if pneumatic-controlled), or width between guide/skirt boards if present. The slope resistance is the resistance caused by incline or decline of the conveyor section:

$$F_{st} = \frac{gLT(t)\sin(\delta)}{V(t)} \quad (4)$$

where g is acceleration due to gravity. Finally, the special resistance is the frictional resistance between the material and guide/skirt boards in the carry-through region. If we make a few reasonable assumptions listed in [7], such as no tilting of the idlers, the following equation is used:

$$F_S = \frac{\mu gLT(t)}{\rho(t)b_1(t)^2V(t)} \quad (5)$$

where μ is the kinetic friction coefficient between the material and guide boards. For friction coefficients, densities and other material constants, user-selected dropdown menus are featured within the tool to assign values from the Engineering Toolbox database [27].

To calculate idler unit masses (Q_{RO} or Q_{RU}), the tool uses the idler spacing (x_{RO} or x_{RU}), width (b_{RO} or b_{RU}), inner and outer diameters ($d_{i\text{-}RO}$, $d_{o\text{-}RO}$ or $d_{i\text{-}RU}$, $d_{o\text{-}RU}$), density (ρ_{RO} or ρ_{RU}), coating

thickness ($t_{c\text{-}RO}$ or $t_{c\text{-}RU}$), and coating density ($\rho_{c\text{-}RO}$ or $\rho_{c\text{-}RU}$) and assumes the rotating part of the idlers is a uniform cylinder:

$$Q_R = \frac{\pi b_R}{4x_R}\left(\rho_R\left({d_{o-R}}^2 - {d_{i-R}}^2\right) + \rho_{c-R}\left((d_{o-R} + 2t_{c-R})^2 - {d_{o-R}}^2\right)\right) \quad (7)$$

The conveyor energy modeling tool outputs the frictional resistances, resultant torque, and rotational velocity at each timestep to calculate power. This is done by fitting a quartic, two-dimensional regression surface to the motors' performance data on an axis orthogonal to RPM and torque, which is considered a standard and reliable method used for curve-fitting dynamometer performance data in industry. The daily energy consumption is then calculated from integrating across the operation profile. Similarly, the yearly energy consumption is calculated from integrating daily energy across a yearly operation schedule.

2.3 Pump Modeling Analysis Procedure

The pump-motor model estimates various speeds and torques from different flowrates and pressure heads that the motor might have to provide in a modeled pump system. The required input motor power is calculated from the stated liquid mass flowrate and pressure head using standard hydraulic equations shown below. The hydraulic power P_h (kW) required by the pump to deliver a volumetric flowrate Q (m^3/h) with density ρ (kg/m^3) for pressure head of h (m) is:

$$P_h = \frac{Q \times \rho \times g \times h}{3.6 \times 10^6} \quad (8)$$

Shaft Power P_s (kW) is used to estimate the motor output power that is delivered to the input of the pump:

$$P_s = \frac{P_h}{\eta_p} \quad (9)$$

For this study, the pump efficiency η_p was estimated to be held constant at 70%. In reality, this efficiency depends on the manufacturer's pump curves and its operating point, but this efficiency was held constant in this study for the purposes of assessing the savings by the motor technology, and not a pump. The torque T_m (N.m) provided by the motor can be calculated by the following equation, where *n* represents the shaft revolutions per minute (rpm):

$$T_m = \frac{9549 \times P_s}{n} \quad (10)$$

Motor input power (kW) is calculated from the shaft power and the motor efficiency, which is calculated by the 2D, fourth-order regression surface fit to the baseline and the proposed retrofit motors' performance curves:

$$P_m = \frac{P_s}{\eta_p} \quad (11)$$

Yearly savings are estimated by integrating time spent by the pump system under the different operating conditions described in the two "distribution" scenarios modeled. The first case included an even distribution of hours across all of the operating points. The second case had an

uneven distribution with some points consisting of a larger share of hours in the year. The distribution of hours at each torque and motor speed in the "uneven distribution" scenario is outlined in Figure 4. Results are provided in the following section, which show that the yearly energy savings are highly dependent on the yearly load profile of the pump installed at the site.

3 Results

The results of both project phases are provided in the following sections. Section 3.1 contains the results of the dynamometer performance characterization with the ZEUS RF-sPMAC motor compared directly to the baseline induction motor. Efficiencies are reported at each speed with respect to torque, as well as across a contour map. Section 3.2 shows the phase 2 results in which energy savings between the two motor and drives was calculated by comparing the estimated energy consumption between the two motor and drives. Section 3.2.1 provides the energy savings estimate in an example conveyor system, and Section 3.2.2 provides the energy savings estimate in an example pump system.

3.1 Laboratory Performance Characterization Results

The resultant dynamometer performance characterization data of the two motor and drive systems at each speed is shown in Figures 7–11. Error bars denote propagated uncertainty in each efficiency measurement. A tabulated form of the data shown at each speed and torque setpoint is also provided in Appendix A. The uncertainty in each base measurement is equivalent to the accuracies specified in Table 6, which generated a mean propagated uncertainty of 0.249% in the efficiency measurement. When using open loop torque control to shift between torque at constant speeds, this prevented the system from stabilizing to the three lowest torque setpoints at 300 RPM. Therefore, the motor efficiencies at these three setpoints were interpolated to a 2D fourth-order regression surface to the other data points like the process used for the Allen Bradley inverter efficiencies described in Section 2.1.

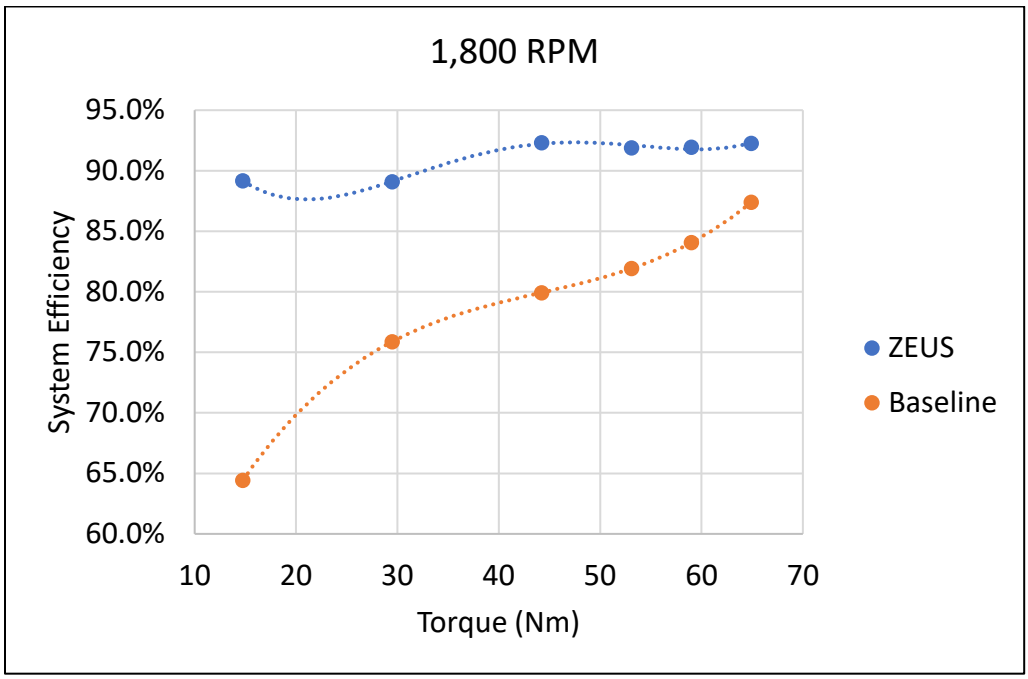

Figure 7. Energy-efficient ZEUS RF-sPMAC vs. baseline motor and drive efficiency with respect to torque (Nm) at rated 1,800 RPM (60 Hz)

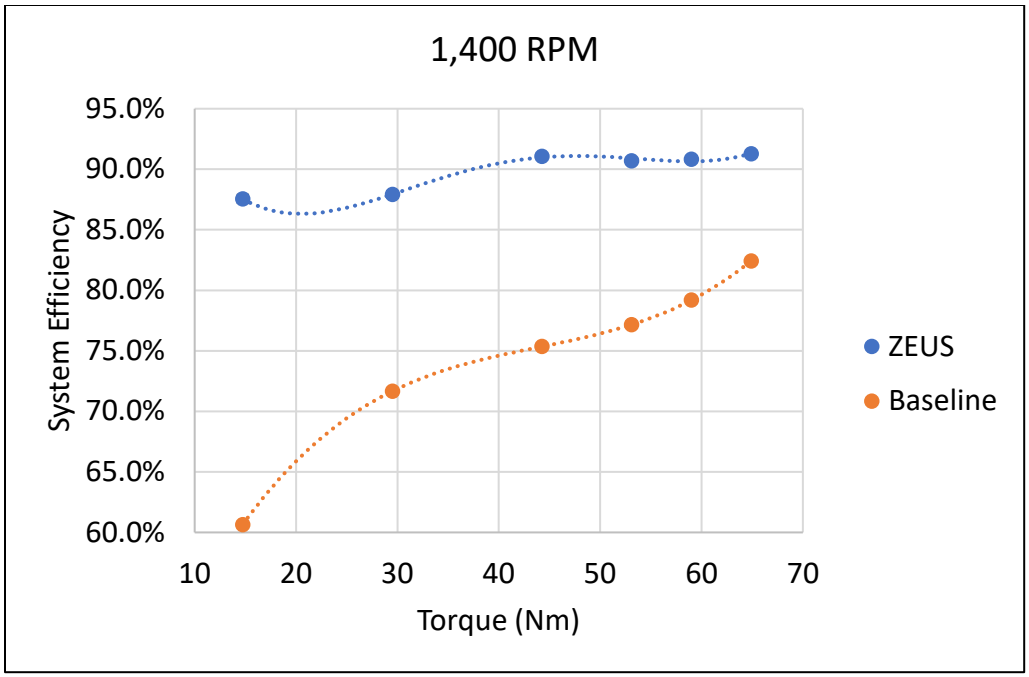

Figure 8. Energy-efficient ZEUS RF-sPMAC vs. baseline motor and drive efficiency with respect to torque (Nm) at 1,400 RPM (46.7 Hz)

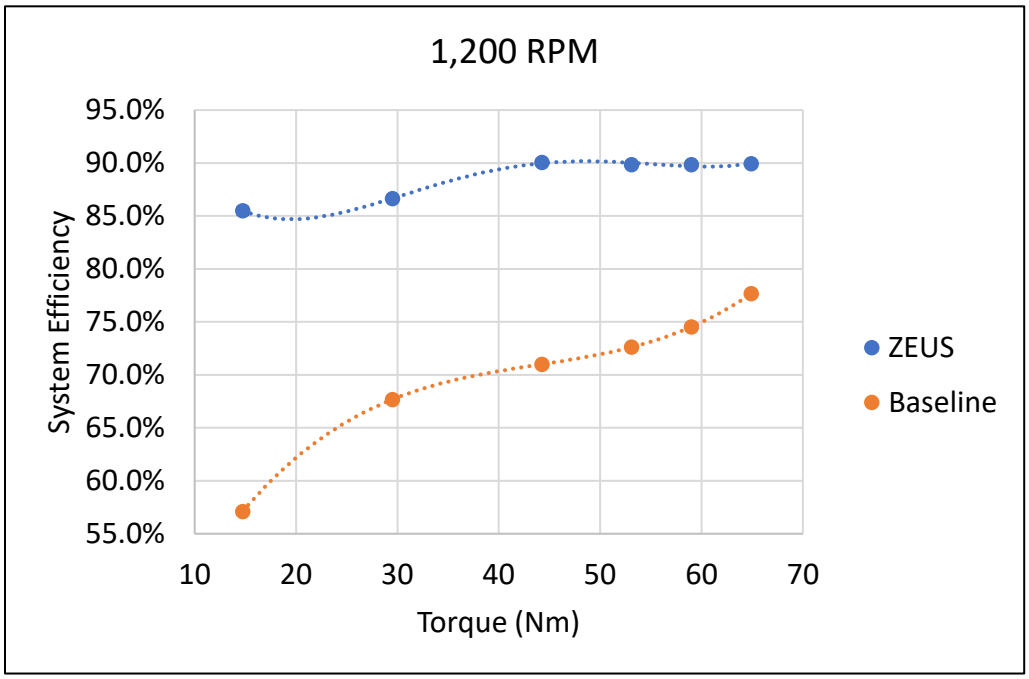

Figure 9. Energy-efficient ZEUS RF-sPMAC vs. baseline motor and drive efficiency with respect to torque (Nm) at rated 1,200 RPM (40 Hz)

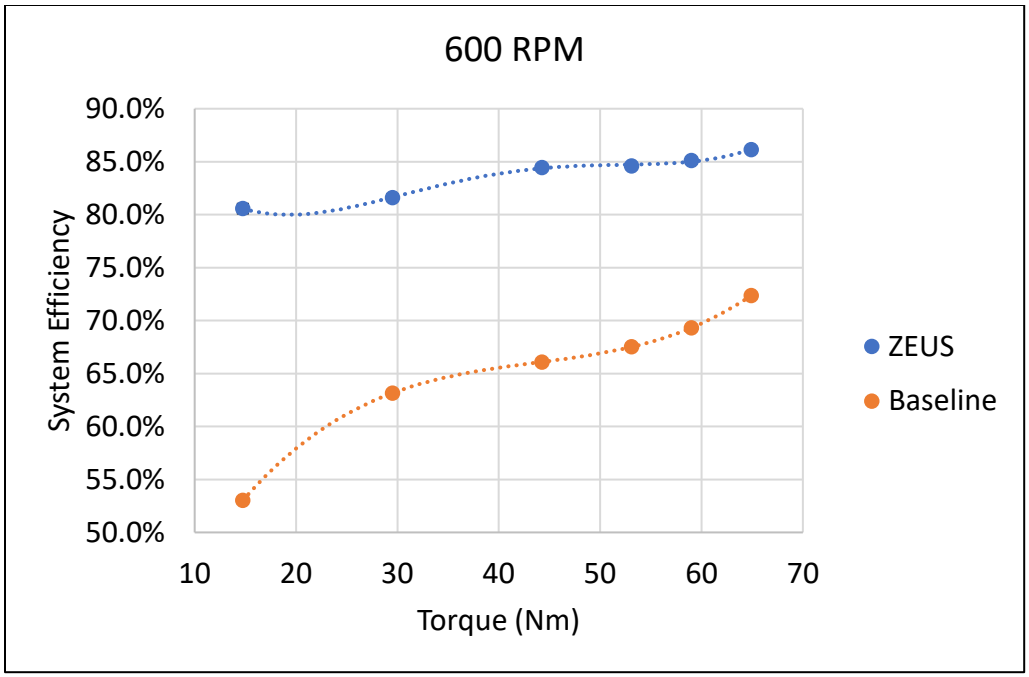

Figure 10. Energy-efficient ZEUS RF-sPMAC vs. baseline motor and drive efficiency with respect to torque (Nm) at 600 RPM (20 Hz)

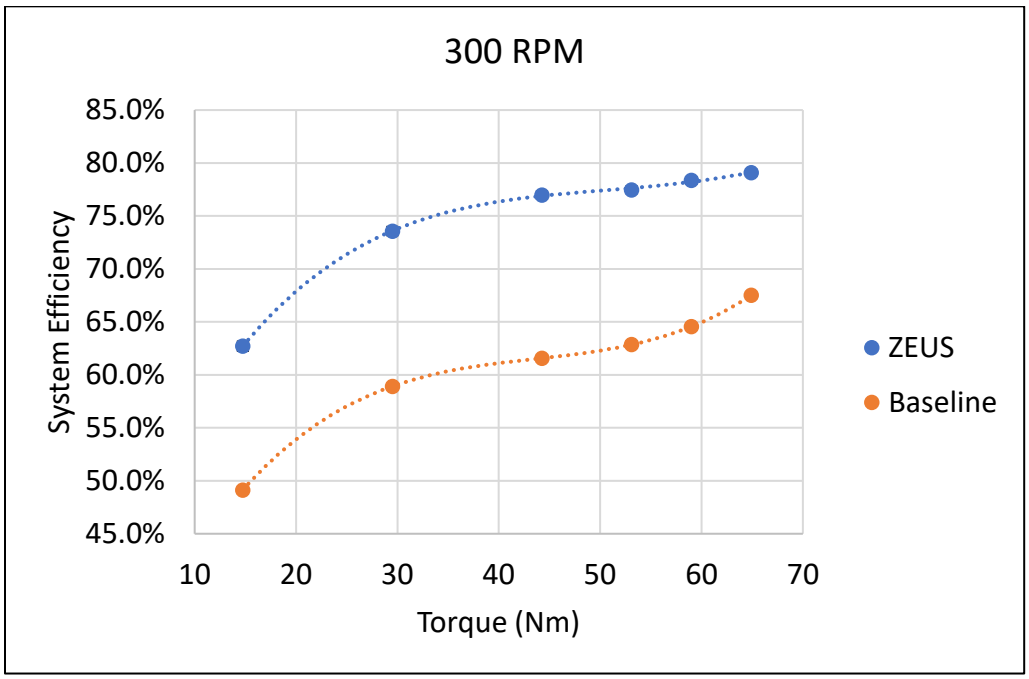

Figure 11. Energy-efficient ZEUS RF-sPMAC vs. baseline motor and drive efficiency with respect to torque (Nm) at 300 RPM (10 Hz)

Figures 7– 11 reveal drastically higher efficiencies observed by the ZEUS RF-sPMAC motor and VFD compared to the baseline induction motor and drive. Significantly improved performance is seen at every torque load and rotational velocity setpoint, although the benefit of the RF-sPMAC motor varies with setpoint. At 110% torque load (64.9 Nm) and rated speed of the motor (60 Hz,

1,800 RPM), the ZEUS RF-sPMAC efficiency was 92.28%, whereas the baseline motor was 87.41% efficient (4.87% improvement). As the torque load was dropped to 25% at the rated speed (14.7 Nm), the benefit of the ZEUS RF-sPMAC was further highlighted. Here, the motor and VFD exhibited 89.18% efficiency whereas the baseline efficiency dropped to 64.44% (24.74% efficiency improvement).

As the speed was reduced, the ZEUS motor and drive's efficiency was found to exhibit significantly reduced losses compared to the baseline motor and drive, which was expected due to the features of its design. At 300 RPM and 110% torque (64.9 Nm), the ZEUS efficiency was reduced to 79.09%, whereas the baseline was reduced to 67.52%, yielding 11.57% improvement. At this low speed, there was diminishing returns as the torque was reduced, reaching only a 13.6% improvement in efficiency by the ZEUS motor and drive at 25% full-load (14.7 Nm). Here, the ZEUS motor and drive efficiency was 62.71% when the baseline only exhibited 49.13% efficiency.

Between these setpoints, there was one point in which the efficiency benefits of the ZEUS motor and drive were maximized compared to the baseline. This occurred at 1,200 RPM at the lowest torque load setpoint (14.7 Nm). Here, the ZEUS RF-sPMAC motor and drive had a system efficiency of 85.48% while the baseline had a mere efficiency of 57.11%. This yielded a maximum efficiency improvement of 28.38%. By observing contour maps of the motor and drive system efficiency with respect to speed and torque, it is much more apparent as to why the greatest benefit of the ZEUS motor occurs at this setpoint. Contour maps of the two motor and drive systems' performance characterizations are shown in Figures 12 and 13. Here, the drastic reduction in efficiency by the baseline motor near 25% torque load can be observed where there is no such reduction in the ZEUS RF-sPMAC motor.

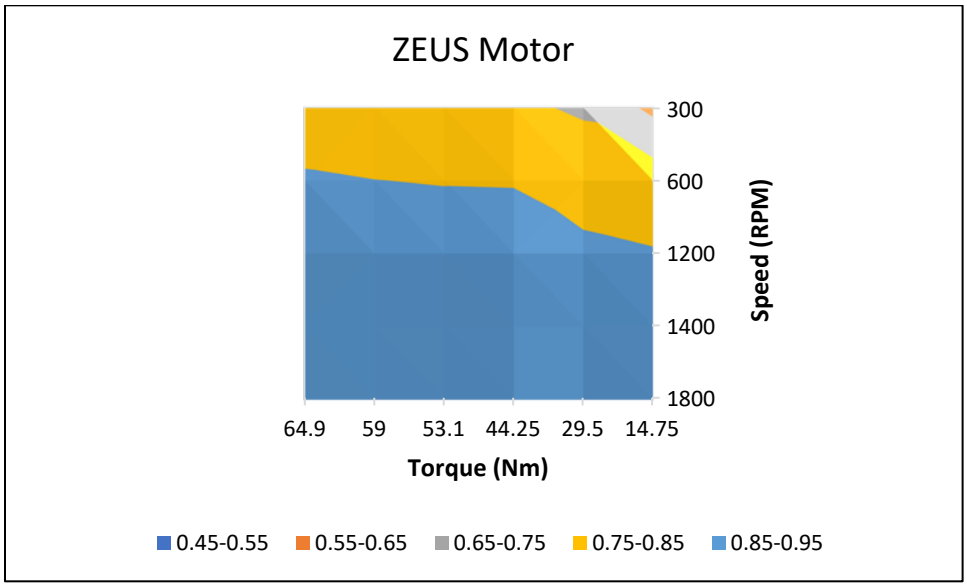

Figure 12. Contour map of the ZEUS RF-sPMAC motor and drive system efficiency from dynamometer performance characterization

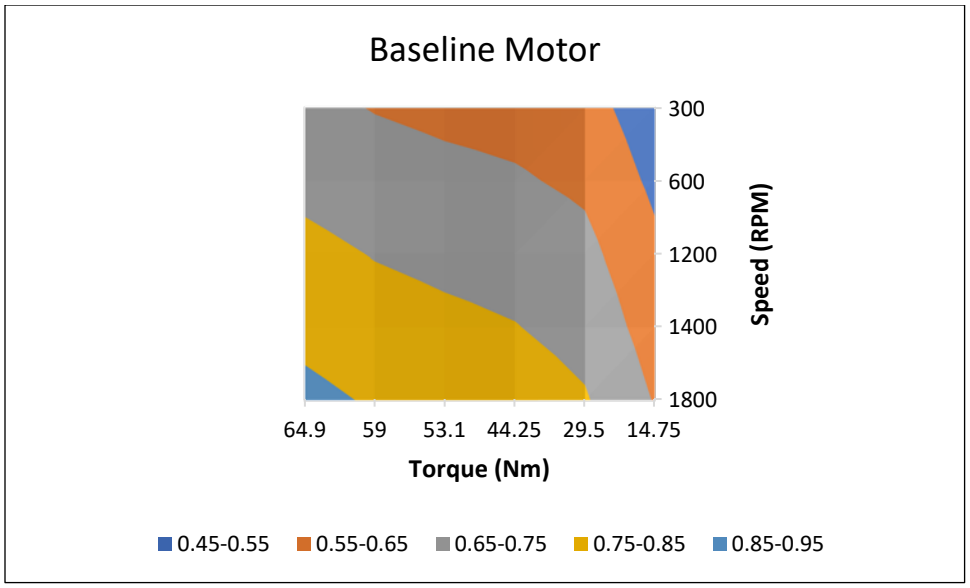

Figure 13. Contour map of the baseline motor and drive system efficiency from manufacturer performance data [2]

These figures illustrate the extraordinary efficiency of the ZEUS Motor system when compared with a NEMA premium induction motor. Based on the differing changes in efficiencies observed between ZEUS RF-sPMAC and baseline motor and drive systems, we can expect the energy savings to vary considerably depending on the manner in which torque, and in some cases, speed, changes throughout operation of a system in which the motor and drives are integrated. Reasonably estimating the energy savings introduced by retrofitting the ZEUS RF-sPMAC motor to systems containing the baseline motor is necessary to accurately predict savings. The energy savings estimates for both the conveyor and pump systems are therefore provided in the upcoming sections.

3.2 Energy Saving Estimate Modeling Results

The ZEUS RF-sPMAC motor and the baseline induction motor were compared in the example conveyor and pump systems listed in sections 1.2.1 and 1.2.2. Again, the demand and energy savings were evaluated in a model of these systems by calculating the speed and torque demand by the conveyor and pump, and then interpolating to the motor and drives' dynamometer performance map. Both the conveyor and pump systems were evaluated under "high speed/high torque," "high speed/low torque," "low speed/high torque," and "low speed/low torque" scenarios. The results of the conveyor analysis are provided in the following Section 3.2.1. The results of the pump analysis are provided in Section 3.2.2.

3.2.1 Example Conveyor System Energy Saving Results

After inputting the ZEUS RF-sPMAC motor and baseline motor data, and the conveyor parameters listed in Table 2 into the conveyor modeling tool described in Ref. [7], the torque and speeds were calculated across the operation day shown in Table 3. Because speed was held constant under each speed/torque scenario, only the torque changed across the operation day due to changes in the material feed rate. The resultant torque profiles across 24-hours for the "high

speed/high torque" and "high speed/low torque" scenarios are shown in Figures 14 and 15, respectively.

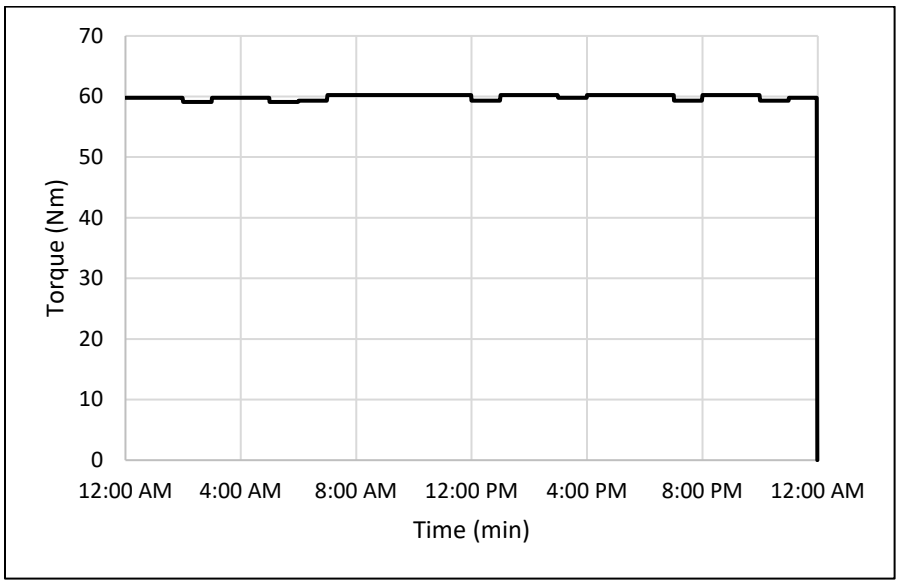

Figure 14. Conveyor torque profile vs. operation time under "high torque" scenario

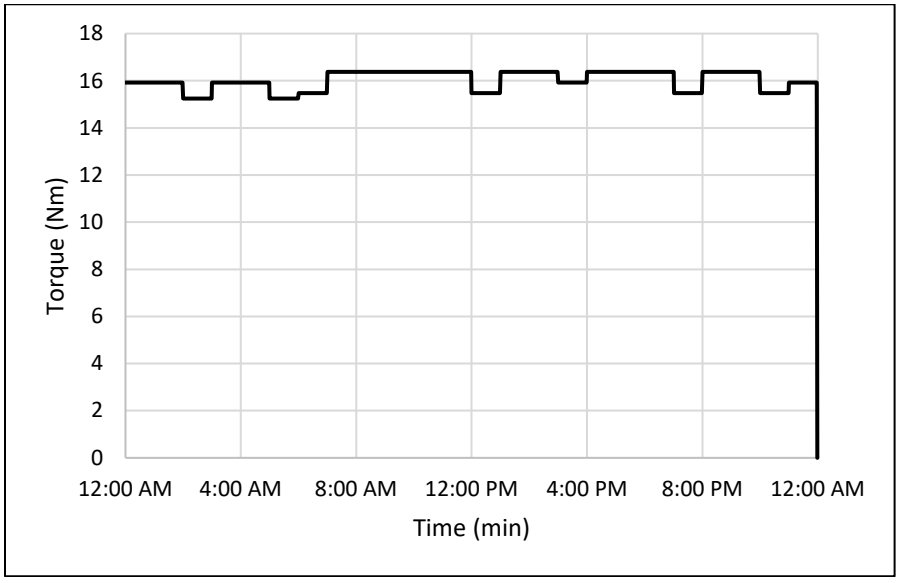

Figure 15. Conveyor torque profile vs. operation time under "low torque" scenario

In Figure 14, the average torque was 60.0 Nm across the 24-hr operation. In Figure 15, the average torque was 16.0 Nm across the 24-hr operation. These average torques only occurred at high speeds or 30 feet/second, because speed also affected torque according to equations 1–6. At low speed (2 ft/second), torque was 48.5 Nm and 24.5 Nm under "high torque" and "low torque" scenarios, respectively. The torque values at each time step under these two "low-speed" scenarios scale proportionally to the torques observed between the two "high speed" scenarios in Figures 14 and 15, respectively, and therefore are not shown. A summary of the average torques and speeds is provided in Table 7.

Table 7. Summary of Average Torque Demand and Motor Speed Under Each Modeling Scenario

	Wide Idler Spacing = 8 m	Short Idler Spacing = 0.8 m
Belt Speed = 2 ft/s	Torque = 24.5 Nm Speed = 114.6 RPM	Torque = 48.5 Nm Speed = 114.6 RPM
Belt Speed = 30 ft/s	Torque = 16.0 Nm Speed = 1,719 RPM	Torque = 60.0 Nm Speed = 1,719 RPM

High Speed/High Torque Scenario

At the highest speed and torque scenario (30 ft/s belt speed, 0.8 m idler spacing), the average torque and belt speed were 60.0 Nm and 1,719 RPM. When interpolated to the performance map of the two motors, the motor and drive system efficiencies were 91.9% and 83.4% for the ZEUS RF-sPMAC and baseline motors, respectively. The average power consumption was then calculated at 11.7 kW for the RF-sPMAC motor and 12.9 kW for the baseline, resulting in 1.20 kW average power reduction. The transient system efficiency and power consumption by the two motors are shown in Figures 16 and 17, respectively:

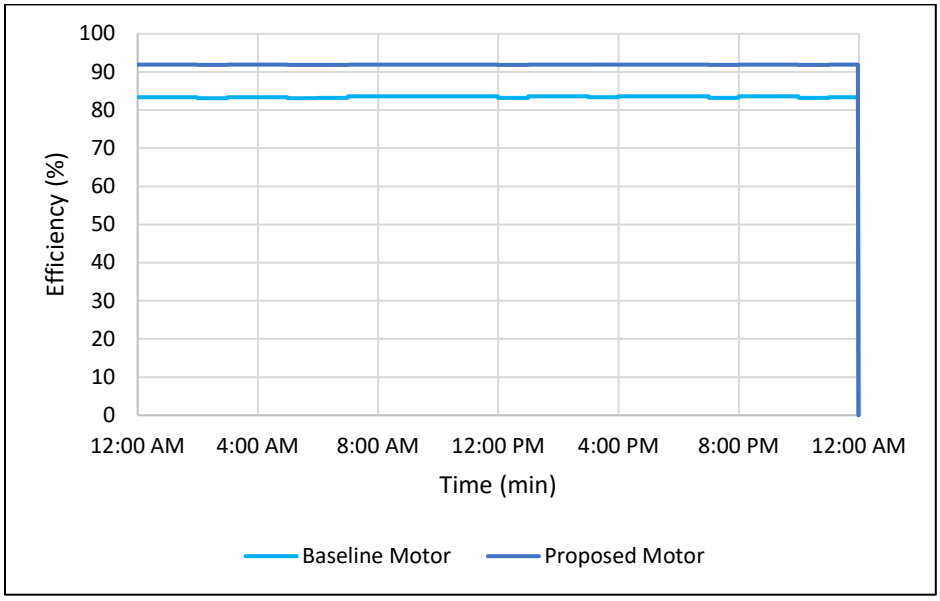

Figure 16. Transient system efficiency of motor/drives under "high speed/high torque" scenario

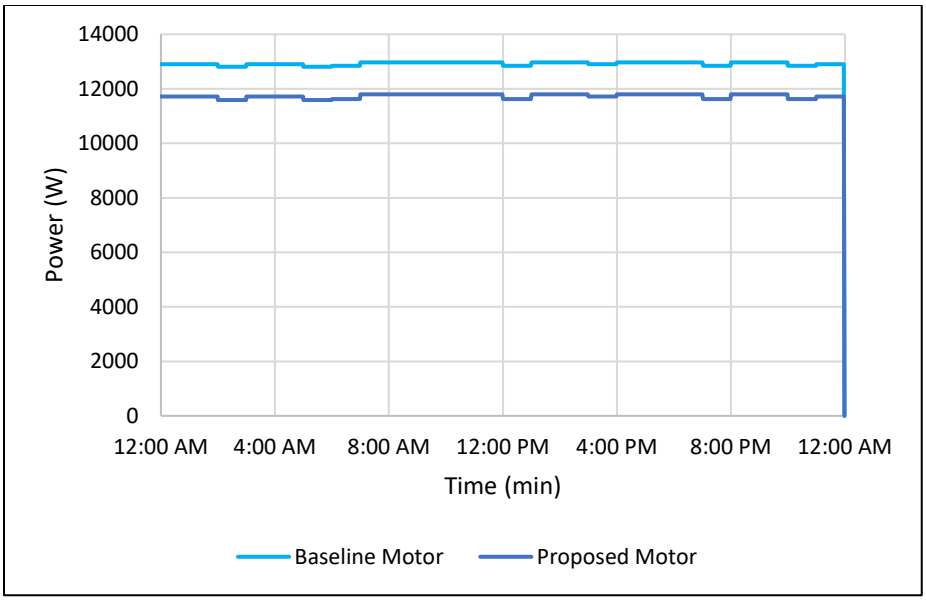

Figure 17. Transient power consumption of motor/drives under "high speed/high torque" scenario

By integrating power across the conveyor's daily operation profile, the ZEUS RF-sPMAC motor and drive was found to consume 281.4 kWh/day, whereas the baseline consumed 309.9 kWh/day. This yielded 28.5 kWh/day energy savings, or 9.20%. When integrated yearly, we assumed that the conveyor operation profile was repeated all 365 days of the year. This resulted in 102.7 MWh yearly energy consumption by the ZEUS RF-sPMAC motor, and 113.1 MWh by the baseline, yielding 10.4 MWh energy savings. At a 16¢/kWh utility rate, this would amount to $1,664.31 of savings. A summary of the mean power and daily and yearly energy and savings is provided in Table 8.

Table 8. Summary of Mean Power and Energy Savings Under "High Speed/High Torque" Scenario

	Mean Power (kW)	Daily Energy (kWh)	Yearly Energy (MWh)
ZEUS RF-sPMAC Motor/Drive	11.73	281.4	102.7
Baseline Motor/Drive	12.92	309.9	113.1
Savings Δ	1.188	28.50	10.40
Savings %		9.20%	

High Speed/Low Torque Scenario

At the high speed and low torque scenario (30 ft/s belt speed, 8 m idler spacing), the average torque and belt speed were 16.0 Nm and 1,719 RPM. When interpolated to the performance map of the two motors, the motor and drive system efficiencies were 88.6% and 65.1% for the ZEUS RF-sPMAC and baseline motors, respectively. The average power consumption was then calculated at 3.26 kW for the RF-sPMAC motor and 4.43 kW for the baseline, resulting in 1.17 kW average power reduction. The transient system efficiency and power consumption by the two motors are shown in Figures 18 and 19, respectively:

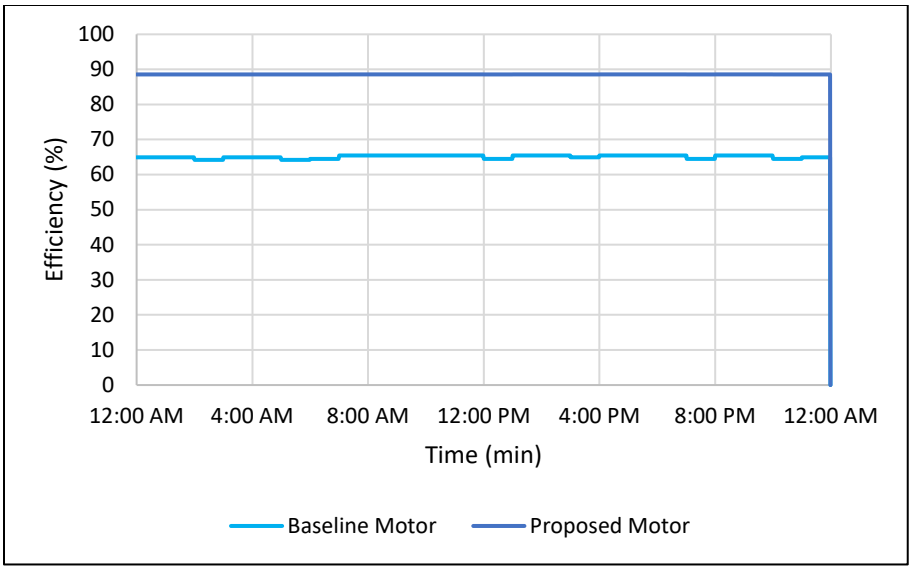

Figure 18. Transient system efficiency of motor/drives under "high speed/low torque" scenario

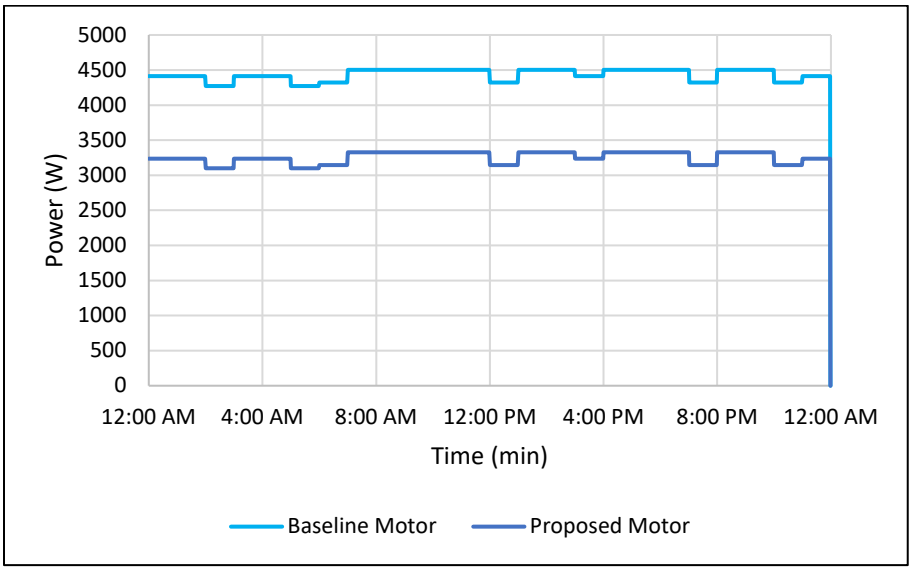

Figure 19. Transient power consumption of motor/drives under "high speed/low torque" scenario

By integrating power across the conveyor's daily operation profile, the ZEUS RF-sPMAC motor and drive was found to consume 78.1 kWh/day, whereas the baseline consumed 106.3 kWh/day. This yielded 28.2 kWh/day energy savings, or 26.5%. Integrating yearly energy consumption resulted in 28.5 MWh yearly energy consumption by the ZEUS RF-sPMAC motor, and 38.8 MWh by the baseline, yielding 10.3 MWh energy savings. At a 16¢/kWh utility rate, this would amount to $1,646.36 of savings, which was nearly the same as under the high speed/high torque scenario. This highlighted the fact that at the motors' rated speed, minimal losses occurred as torque is reduced. A summary of the mean power and daily and yearly energy and savings is provided in Table 9.

Table 9. Summary of Mean Power and Energy Savings Under "High Speed/Low Torque" Scenario

	Mean Power (kW)	Daily Energy (kWh)	Yearly Energy (MWh)
ZEUS RF-sPMAC Motor/Drive	3.256	78.08	18.50
Baseline Motor/Drive	4.431	106.3	38.79
Savings Δ	1.175	28.19	10.29
Savings %	26.5%		

Low Speed/High Torque Scenario

At the low speed and high torque scenario (2 ft/s belt speed, 0.8 m idler spacing), the average torque and belt speed were 48.5 Nm and 114.6 RPM. When interpolated to the performance map of the two motors, the motor and drive system efficiencies were 69.0% and 58.7% for the ZEUS RF-sPMAC and baseline motors, respectively. The average power consumption was then calculated at 843 W for the RF-sPMAC motor and 991 W for the baseline, resulting in 148 W average power reduction. The transient system efficiency and power consumption by the two motors are shown in Figures 20 and 21, respectively:

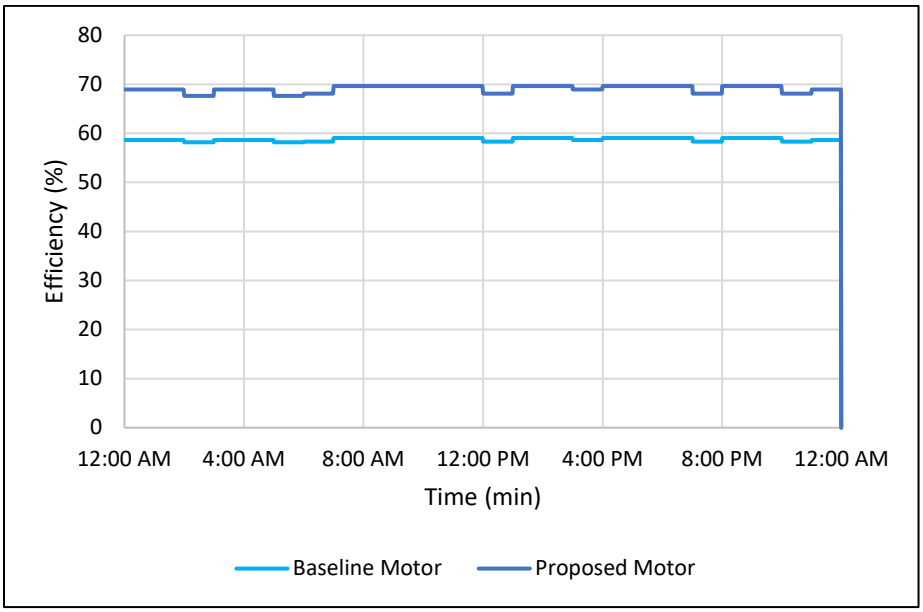

Figure 20. Transient system efficiency of motor/drives under "low speed/high torque" scenario

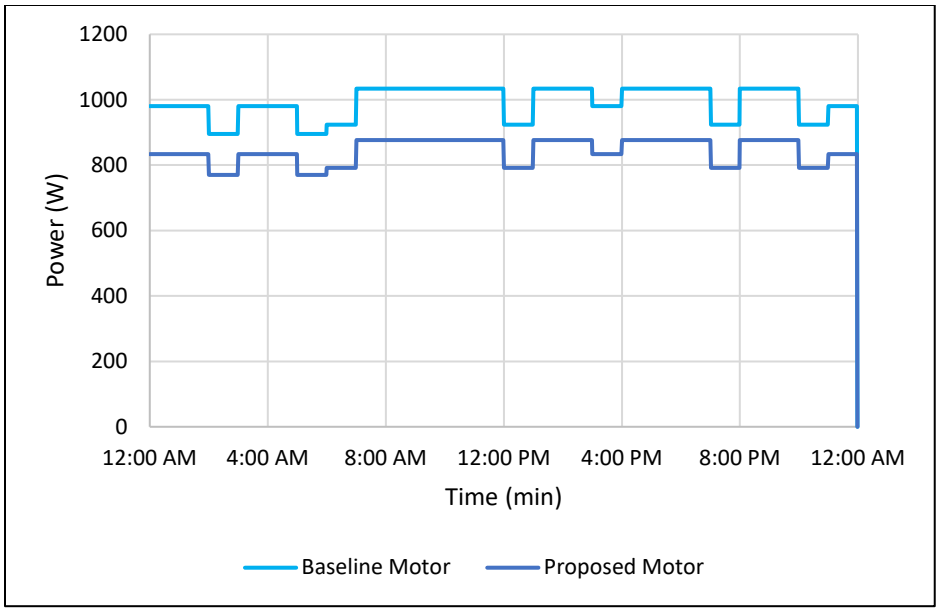

Figure 21. Transient power consumption of motor/drives under "low speed/high torque" scenario

By integrating power across the conveyor's daily operation profile, the ZEUS RF-sPMAC motor and drive was found to consume 20.2 kWh/day, whereas the baseline consumed 23.8 kWh/day. This yielded 3.54 kWh/day energy savings, or 14.9%. Yearly energy resulted in 7.38 MWh consumption by the ZEUS RF-sPMAC motor, and 8.67 MWh by the baseline, yielding 1.29 MWh energy savings. At a 16¢/kWh utility rate, this would amount to $206.85 of savings. A summary of the mean power and daily and yearly energy and savings is provided in Table 10.

Table 10. Summary of Mean Power and Energy Savings Under "Low Speed/High Torque" Scenario

	Mean Power (kW)	Daily Energy (kWh)	Yearly Energy (MWh)
ZEUS RF-sPMAC Motor/Drive	0.8431	20.22	7.380
Baseline Motor/Drive	0.9908	23.76	8.673
Savings Δ	0.1477	3.542	1.293
Savings %	14.9%		

Low Speed/Low Torque Scenario

At the low speed and low torque scenario (2 ft/s belt speed, 8 m idler spacing), the average torque and belt speed were 24.5 Nm and 114.6 RPM. This speed/torque yielded motor and drive system efficiencies of 59.6% and 53.5% for the ZEUS RF-sPMAC and baseline motors, respectively. The average power consumption was then calculated at 492 W for the RF-sPMAC motor and 547 W for the baseline, resulting in 55.7 W average power reduction. The transient system efficiency and power consumption by the two motors are shown in Figures 22 and 23, respectively:

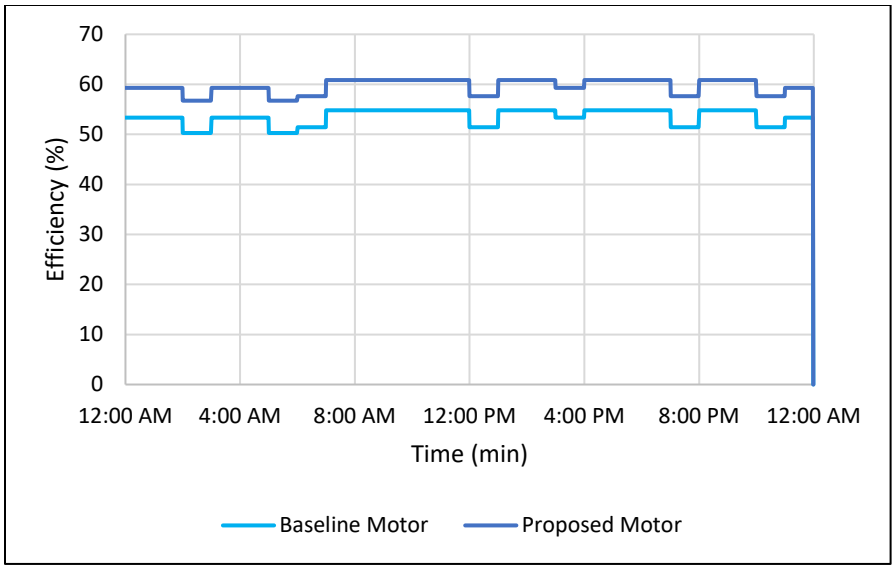

Figure 22. Transient system efficiency of motor/drives under "low speed/low torque" scenario

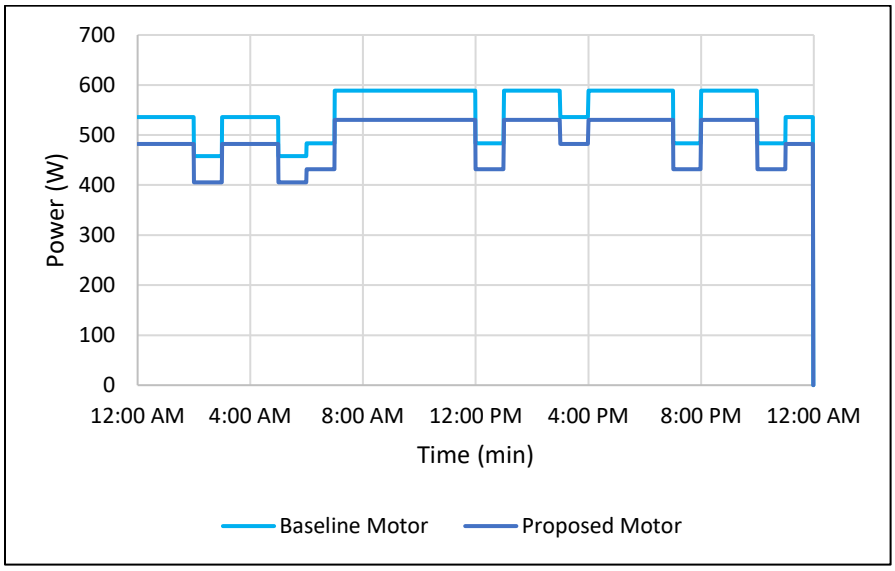

Figure 23. Transient power consumption of motor/drives under "low speed/low torque" scenario

The ZEUS RF-sPMAC motor and drive consumed 11.8 kWh/day when power was integrated across the conveyor's daily operation profile, whereas the baseline consumed 13.1 kWh/day. This yielded 1.34 kWh/day energy savings, or 10.2%. Yearly energy resulted in 4.30 MWh consumption by the ZEUS RF-sPMAC motor, and 4.79 MWh by the baseline, which yielded 0.488 MWh energy savings. At a 16¢/kWh utility rate, this would amount to $78.03 of energy savings. A summary of the mean power and daily and yearly energy and savings is provided in Table 11.

Table 11. Summary of Mean Power and Energy Savings Under "Low Speed/Low Torque" Scenario

	Mean Power (kW)	Daily Energy (kWh)	Yearly Energy (MWh)
ZEUS RF-sPMAC Motor/Drive	0.4915	11.79	4.302
Baseline Motor/Drive	0.5472	13.12	4.790
Savings Δ	0.0557	1.336	0.4877
Savings %	10.2%		

Summary

Under the "high speed/high torque" scenario, the percent energy savings was at its minimum of the four scenarios analyzed. This was expected, considering the fact that efficiency gain by the ZEUS RF-sPMAC motor vs. the baseline was at its minimum here. As the speed and torque were reduced, percent energy savings increased and then again dropped off at the "low speed/low torque" scenario. Percent savings increased more dramatically with reduced torque than reduced speed. This was due to the reduced losses with respect to torque in the ZEUS RF-sPMAC motor compared to the baseline, which can be observed in Figures 12 and 13. Despite this, the absolute value of the energy savings was at its maximum under the "high speed/high torque" scenario. This is because although the percent energy savings was lowest here, larger percentages of savings seen at lower speeds and torques constitute a fraction of significantly reduced baseline demand. It is also important to note that savings was nearly the same between high and low torques when operating at high speed. This highlighted the fact that at the motors' rated speed, minimal losses occur regardless of the operating torque.

When analyzing the energy consumption and savings of a conveyor system, it is often useful to analyze the savings in per tons*mile. This allows a conveyor operator to determine the energy needed per the amount of conveyed material processed. The conveyor moves 32.73 miles per day under low-speed scenarios, and 490.9 miles per day under high-speed scenarios. By integrating daily the hourly feed rate onto the conveyor provided in Table 3, we find that the total daily mass fed is 163.24 tons. Therefore, we have 5,342.4 ton*miles of material conveyed under low-speed scenarios, and 80,136 ton*miles conveyed under high-speed scenarios. It should be noted that the majority of energy used by a conveyor does not come from the torque required to move the material, however. Conveyors are designed so that most of the torque is required to rotate the idler rollers and pull the belt [7]. The torque contribution by the material is a small fraction because otherwise if the feed rate was altered considerably, then the torque might swing outside of the motor and drive's operation range. The overall energy/ton*mile consumed, which is shown in Table 12 below, therefore does not scale to conveyed tons*miles:

Table 12. Energy/Ton*Mile Consumption and Savings at Each Speed/Torque Scenario

	ZEUS RF-sPMAC Motor/Drive	Baseline Motor/Drive	Savings Δ
High Speed / High Torque	3.51 Wh/ton*mile	3.87 Wh/ton*mile	0.360 Wh/ton*mile

	ZEUS RF-sPMAC Motor/Drive	Baseline Motor/Drive	Savings Δ
High Speed / Low Torque	0.974 Wh/ton*mile	1.33 Wh/ton*mile	0.352 Wh/ton*mile
Low Speed / High Torque	0.252 Wh/ton*mile	0.296 Wh/ton*mile	0.044 Wh/ton*mile
Low Speed / Low Torque	0.147 Wh/ton*mile	0.164 Wh/ton*mile	0.0167 Wh/ton*mile

3.2.2 Example Pump System Energy Saving Results

Table 13 displays the number of hours that the two motors were subjected to the torque, T_M (Nm) and shaft speed, V (RPM) in each of the two scenarios. The two assumed load scenarios for the pump system model were applied to the equations listed in Section 2.3 to calculate instantaneous power, which was integrated across the scenario profile to predict energy use. The first scenario was the "even" distribution scenario in which daily hours at constant flowrate and pressure head conditions were evenly distributed across the year. Under the second, the "uneven" distribution scenario, different flowrates and pressure heads were variably distributed across the daily operation profile according to Figure 4. The yearly working hours were calculated using 12-hour days for 5 days per week, with 52 weeks per year for a total of 3,120 hours out of 8,760 possible yearly hours.

Table 13. Load profile at Each Speed/Torque Scenario (T_M: Nm, V: RPM)

Condition		Uneven distribution (hours)	Even Distribution (hours)
T_M:58.85	V:1,800	31.2	156
T_M:58.85	V:1,620	62.4	156
T_M:58.85	V:1,440	62.4	156
T_M:58.85	V:1,260	93.6	156
T_M:58.85	V:1,080	93.6	156
T_M:47.08	V:1,800	156	156
T_M:47.08	V:1,620	218.4	156
T_M:47.08	V:1,440	312	156
T_M:47.08	V:1,260	312	156
T_M:47.08	V:1,080	218.4	156
T_M:35.31	V:1,800	156	156
T_M:35.31	V:1,620	218.4	156
T_M:35.31	V:1,440	312	156
T_M:35.31	V:1,260	312	156
T_M:35.31	V :1,080	218.4	156
T_M:23.54	V :1,800	31.2	156
T_M:23.54	V:1,620	62.4	156
T_M:23.54	V:1,440	62.4	156
T_M:23.54	V:1,260	93.6	156
T_M:23.54	V:1,080	93.6	156

When applied to the hydraulic equations in Section 2.3, the torque and motor velocities across the prescribed number of "even" distribution scenario hours yielded a power demand of 8.15 kW in the baseline induction motor, yet only 6.88 kW in the ZEUS RF-sPMAC motor and drive. This constituted a power reduction of 15.6%. In the "uneven" distribution scenario, the torque and motor speed varied but averaged to a resultant 7.99 kW power consumption in the baseline induction motor, yet only 6.69 kW in the RF-sPMAC, which constituted a 16.3% reduction. As the torque and velocity varied in the "uneven" distribution scenario, the resulting power consumption by the two motors changed respectively. A profile of the demand on both the baseline induction and ZEUS RF-sPMAC motor and drives is displayed in Figure 24.

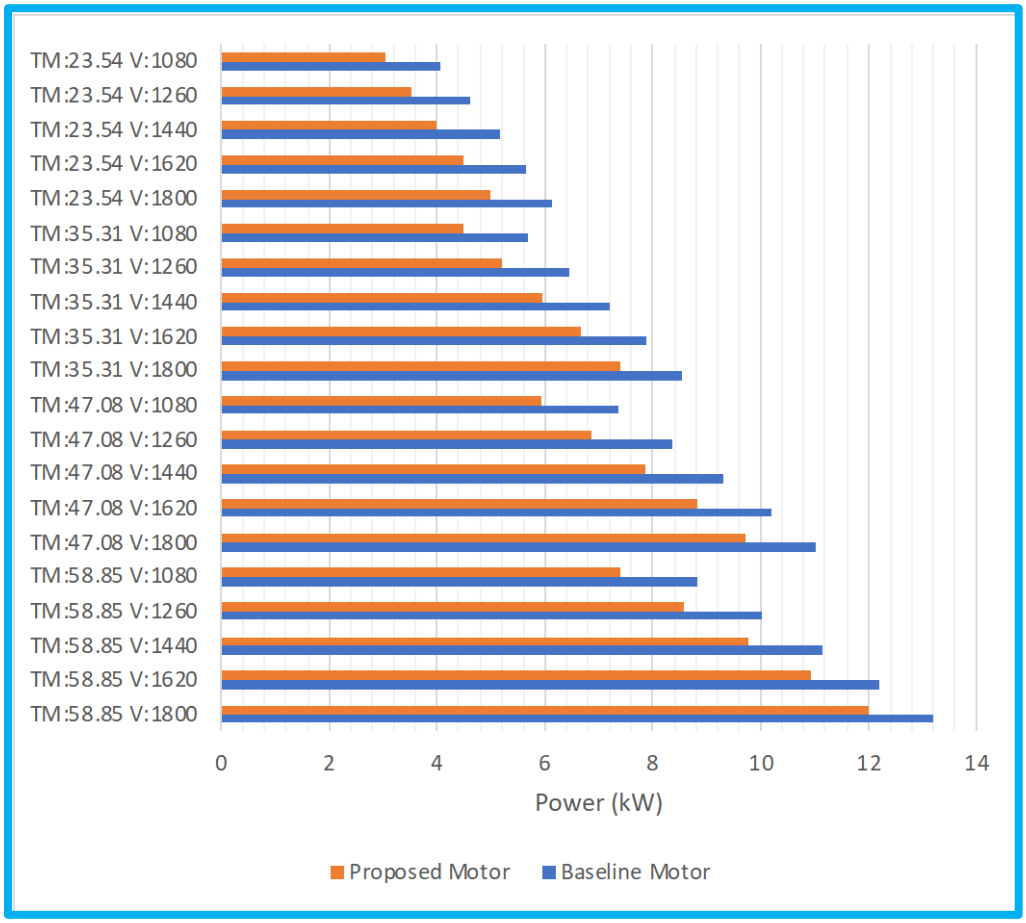

Figure 24. Power consumption of baseline and proposed motor/drives at various torques (tm) and shaft speeds (v)

"Even" Distribution Scenario

Table 14 summarizes the power and energy savings for the "even distribution" scenario, which resulted in 15.6% overall energy savings by the ZEUS RF-sPMAC motor and drive compared to the baseline. The daily energy consumption by the RF-sPMAC was 58.8 kWh whereas the baseline motor/drive consumed 69.7 kWh/day, constituting 10.9 kWh/day savings. The RF-sPMAC motor/drive consumed 21.5 MWh of energy yearly compared to 25.4 MWh by the baseline motor/drive. This constituted 3.97 MWh of yearly savings.

Table 14. Summary of Mean Power and Energy Savings Under "Even Distribution" Scenario

	Mean Power (kW)	Daily Energy (kWh)	Yearly Energy (MWh)
ZEUS RF-sPMAC Motor/Drive	6.88	58.82	21.47
Baseline Motor/Drive	8.15	69.69	25.44
Savings Δ	1.27	10.87	3.965
Savings %	15.6%		

"Uneven" Distribution Scenario

Table 15 summarizes the power and energy savings by the ZEUS RF-sPMAC in the "uneven" distribution scenario, which resulted in 16.3% overall savings. The daily energy consumption in this scenario was 58.8 kWh/day by the RF-sPMAC motor whereas the baseline consumption was 69.7 kWh/day, yielding 10.9 kWh/day of energy savings. The RF-sPMAC motor/drive consumed 20.9 MWh of energy yearly in this scenario, compared to a yearly 24.9 MWh by the baseline condition. This resulted in savings of 24.9 MWh/year.

The energy savings results between the "even" and "uneven" distributions were similar in both the scenarios due to the combined influence of head pressure and flowrate on both motor torque and speed. Varying these two parameters resulted in an outcome of similar mean power demand, but not identical. The energy savings was also not identical because it depends on the load profile for the pump-motor drive configuration. For a tangible savings evaluation in buildings, the model used in this study should be updated with an actual pump load profile to obtain realistic savings for a respective motor-pump setup.

Table 15. Summary of Mean Power and Energy Savings Under "Uneven Distribution" Scenario

	Mean Power (kW)	Daily Energy (kWh)	Yearly Energy (MWh)
ZEUS RF-sPMAC Motor/Drive	6.69	57.17	20.87
Baseline Motor/Drive	7.99	68.32	24.94
Savings Δ	1.3	11.15	4.07
Savings %	16.3%		

Summary

By varying the speed and torque around operation parameters seen in a typical pump system, as was done in the "uneven" distribution scenario, the resulting energy savings deviated from the average observed in the "even" distribution scenario only modestly. However, the savings did increase due to the differences in performance between the RF-sPMAC motor and baseline at different speed/torque points. At higher speeds/torques, there is less significant savings incurred by the RF-sPMAC motor compared to the baseline. At lower speeds/torques, there is however much greater savings. Because the number of hours in the "uneven" distribution that the speeds

and torques were reduced below those used in the “even” distribution scenario was similar to the number of hours increased above those speeds and torques, the greater savings below those speeds and torques will overcome the reduced savings above. Therefore, the average energy savings was greater in the “uneven” distribution.

The difference in energy consumption and savings by the two motors in these scenarios showed that the energy consumption depends significantly on the load profile for the pump-motor drive setup. For a tangible savings evaluation in buildings, the model used in this study should be applied to an actual pump load profile to obtain more realistic savings for respective motor-pump setups.

4 Conclusion

The performance improvement and energy savings potential of a novel 15 HP radial flux, surface permanent magnet AC motor (RF-sPMAC) designed by ZEUS Motor Inc. was evaluated in this study. The results showed that the motor is significantly more efficient than a standard baseline induction motor with equivalent ratings and electrical specifications. In phase 1, an experimental characterization of the ZEUS RF-sPMAC motor and VFD was conducted using a dynamometer in accordance with ANSI/ASHRAE 222-2018 [1] and following the procedures of the ISO 17025-accredited North Carolina Advanced Energy Corporation. The motor was then compared with the manufacturers' performance data of a standard baseline induction motor and VFD with equivalent motor ratings and specifications. In phase 2, the daily and annual energy and demand savings against the baseline were estimated in an example model of a conveyor belt system and building water pump system using formulas derived from ANSI/ISO standard 5048-1989 [6] and standard hydraulic theory pump equations, respectively.

The phase 1 dynamometer characterization revealed motor and drive system efficiencies that were notably higher than one would observe with typical current motors of this size, and significantly higher than the baseline. The maximum efficiency of the ZEUS RF-sPMAC motor and drive was 92.3% at the highest torque load (64.9 Nm) and rated speed (1,800 RPM). The baseline motor was more inhibited by VFD losses, reaching only 87.4% efficiency. The ZEUS RF-sPMAC motor was especially beneficial at low torques, where efficiencies exhibited a minimal reduction compared to the drastic losses seen in an induction motor. At the lowest torque load setpoint (14.7 Nm), and 1,200 RPM speed, the RF-sPMAC saw the maximum efficiency gain of 28.4%. Here, the motor and drive's efficiency was 85.5%, whereas the baseline's was 57.1%.

Conveyor Energy Savings

Modeling conveyor and pump systems in phase 2 involved evaluating the daily and yearly energy savings under parameters that would yield four speed/torque scenarios distributed across the motor and drives' performance range: (A) high speed/high torque, (B) high speed/low torque, (C) low speed/high torque, and (D) low speed/low torque. The energy, mean demand, and cost savings for each scenario in the example conveyor were as follows (cost savings estimated at 16¢/kWh utility rate):

A) 9.20% energy savings: 281.4 kWh/day by the ZEUS RF-sPMAC Motor and 309.9 kWh/day by the baseline resulting in 28.5 ΔkWh/day savings. 102.7 MWh/year by the ZEUS RF-sPMAC Motor and 113.1 MWh/year by the baseline resulting in 10.4 ΔMWh/day savings. 3.51 Wh/ton*mile by the ZEUS RF-sPMAC Motor and 3.87 Wh/ton*mile by the baseline resulting in 0.360 Wh/ton*mile savings. $1,664.31 estimated yearly savings.
B) 26.5% energy savings: 78.1 kWh/day by the ZEUS RF-sPMAC Motor and 106.3 kWh/day by the baseline resulting in 28.2 ΔkWh/day savings. 28.5 MWh/year by the ZEUS RF-sPMAC Motor and 38.8 MWh/year by the baseline resulting in 10.3 ΔMWh/day savings. 0.974 Wh/ton*mile by the ZEUS RF-sPMAC Motor and 1.33 Wh/ton*mile by the baseline resulting in 0.352 Wh/ton*mile savings. $1,646.36 estimated yearly savings.

C) 14.9% energy savings: 20.2 kWh/day by the ZEUS RF-sPMAC Motor and 23.8 kWh/day by the baseline resulting in 3.54 ΔkWh/day savings. 7.38 MWh/year by the ZEUS RF-sPMAC Motor and 8.67 MWh/year by the baseline resulting in 1.29 ΔMWh/day savings. 0.252 Wh/ton*mile by the ZEUS RF-sPMAC Motor and 0.296 Wh/ton*mile by the baseline resulting in 0.044 Wh/ton*mile savings. $206.85 estimated yearly savings.
D) 10.2% energy savings: 11.8 kWh/day by the ZEUS RF-sPMAC Motor and 13.1 kWh/day by the baseline resulting in 1.34 ΔkWh/day savings. 4.30 MWh/year by the ZEUS RF-sPMAC Motor and 4.79 MWh/year by the baseline resulting in 0.488 ΔMWh/day savings. 0.147 Wh/ton*mile by the ZEUS RF-sPMAC Motor and 0.164 Wh/ton*mile by the baseline resulting in 0.0167 Wh/ton*mile savings. $78.03 estimated yearly savings.

With multiple conveyor sections in a typical operation, these savings would multiply by the number of retrofit motor/drive systems. Because the ZEUS RF-sPMAC motor had reduced losses with respect to torque compared to the baseline, percent savings increased as torque was reduced in the conveyor. The overall energy and cost savings, however, diminished as speed was reduced, because the energy used by both motors declined significantly.

Pump Energy Savings

The pump model assumed different operating conditions by varying the required flow rate and pressure head. The yearly operating time at each operating condition was considered in two distinct scenarios: an (A) "even" distribution scenario and a (B) "uneven" distribution scenario. In the former, the pressure head and flowrate were held constant, whereas they were varied across the operation profile in the latter. In this example building pump system, the energy, mean demand, and cost savings for each scenario were as follows (cost savings estimated at 16¢/kWh utility rate):

A) 15.6% overall savings: 58.8 kWh/day by the ZEUS RF-sPMAC Motor and 69.7 kWh/day by the baseline resulting in 10.9 ΔkWh/day savings. 21.5 MWh/year by the ZEUS RF-sPMAC Motor and 25.4 MWh/year by the baseline resulting in 3.97 ΔMWh/year savings and $635 estimated yearly cost savings.
B) 16.3% overall savings: 57.2 kWh/day by the ZEUS RF-sPMAC Motor and 68.3 kWh/day by the baseline resulting in 11.1 ΔkWh/day savings. 20.9 MWh/year by the ZEUS RF-sPMAC Motor and 24.9 MWh/year by the baseline resulting in 4 ΔMWh/year savings and $651 estimated yearly cost savings.

The ZEUS RF-PMAC motor sees these higher efficiencies compared to other PMAC motors due to its design, which uses a stator composed of very tightly packed magnetic steel and copper. This allows the motor size to be reduced such that its internal cavity is 1/30th the size of common induction motors. External cooling is not necessary with this design, which reduces the overall demand and increases efficiency.

References

1. ANSI, A., *Standard Method of Test for Electrical Power Drive Systems*. 2018, ANSI / ASHRAE.
2. *The MotorMaster+ Software Tool*. 2020, U.S. Department of Energy Office of Energy Efficiency & Renewable Energy (EERE) Industrial Technologies Program.
3. *Global Conveyor Belt Market Size By Material, By Product, By End-User, By Geographic Scope And Forecast*. 2020, ESOMAR22 Corporate: Verified Market Research.
4. *About the Commercial Buildings Integration Program*. 2020; Available from: https://www.energy.gov/eere/buildings/about-commercial-buildings-integration-program
5. *Energy use in commercial buildings*. Use of Energy Explained 2018; Available from: https://www.eia.gov/energyexplained/use-of-energy/commercial-buildings.php.
6. ANSI, I., *Continuous mechanical handling equipment - Belt conveyors with carrying idlers - Calculation of operating power and tensile forces*. 1989, ISO.
7. Bulk, A., G. Shoukas, and R. Faramarzi, *Industrial Conveyor Motor Performance Evaluation*. 2021, National Renewable Energy Lab.(NREL), Golden, CO (United States).
8. Hughes, A. and B. Drury, *Electric motors and drives: fundamentals, types and applications*. 2019: Newnes.
9. Kraftmakher, Y., *Demonstration of Lenz's law with an induction motor.* Physics education, 2005. **40**(3): p. 281.
10. Coulter, D., J. Ahmed, T. Pistochini, and C. Mande, *Software-Controlled Switch Reluctance Motors*. 2018, Souther California Edison.
11. Bezesky, D.M. and S. Kreitzer. *NEMA Application Guide for AC adjustable speed drive systems*. in *Record of Conference Papers. IEEE incorporated Industry Applications Society. Forty-Eighth Annual Conference. 2001 Petroleum and Chemical Industry Technical Conference (Cat. No. 01CH37265)*. 2001. IEEE.
12. Pillay, P. and P. Freere. *Literature survey of permanent magnet AC motors and drives*. in *Conference Record of the IEEE Industry Applications Society Annual Meeting*. 1989. IEEE.
13. Parsa, L., *Performance improvement of permanent magnet AC motors*. 2005, Texas A&M University.
14. Klontz, K.W. *Permanent magnet motor with tested efficiency beyond ultra-premium/ie5 levels*. in *Proc. ACEEE Summer Study on Energy Efficiency in Industry*. 2017.
15. Rouse, S. and D. Dederer, *VARIABLE FREQUENCY DRIVES - Energy Efficiency Reference Guide*. 2009, Centre for Energy Advancement through Technological Innovation (CEATI International): Natural Resources Canada.
16. Fang, L., J.-w. Jung, J.-P. Hong, and J.-H. Lee, *Study on high-efficiency performance in interior permanent-magnet synchronous motor with double-layer PM design.* IEEE Transactions on Magnetics. 2008. **44**(11): p. 4393-4396.
17. Sone, K., M. Takemoto, S. Ogasawara, K. Takezaki, and W. Hino. *Examination for the higher efficiency in a ferrite permanent magnet 10 kW in-wheel axial-gap motor with coreless rotor structure*. in *2014 IEEE Energy Conversion Congress and Exposition (ECCE)*. 2014. IEEE.

18. Ullah, K., J. Guzinski, and A.F. Mirza, *Critical review on robust speed control techniques for permanent magnet synchronous motor (PMSM) speed regulation.* Energies, 2022. **15**(3): p. 1235.
19. Energy, A., *Zero E Technologies 15Hp ZEUS Motor™ Testing*. 2016.
20. ZERO-E TECHNOLOGIES, I. *ZEUS MOTORS OUTPERFORM THE REST - THE WORLD'S MOST ENERGY EFFICIENT MOTORS*. 2021; Available from: https://zeusmotor.com/
21. Burt, C.M., X. Piao, F. Gaudi, B. Busch, and N. Taufik, *Electric motor efficiency under variable frequencies and loads.* Journal of Irrigation and Drainage Engineering, 2008. **134**(2): p. 129-136.
22. Wallbom-Carlson, A., *Energy comparison. VFD vs. on-off controlled pumping stations.* Scientific impeller, 1998. **136**(5): p. 29-32.
23. Jinrong, C., W. Shifeng, Z. Zihao, L. Guohua, and L. Xunan, *Determination of the friction coefficient of coal particles by discrete element simulation and experimentation.* 2020.
24. Miskovic, Z., R. Mitrovic, V. Maksimović, and A. Milivojević, *Analysis and prediction of vibrations of ball bearings contaminated by open pit coal mine debris particles.* Tehnicki Vjesnik= Technical Gazette. 2017. **24**(6): p. 1941-1950.
25. Shadid, F. *Average U.S. coal mining productivity increases as production falls*. TODAY IN ENERGY 2018 [cited 2022; Available from: https://www.eia.gov/todayinenergy/detail.php?id=35232
26. Williams, J. *Belt conveyor danger zones*. Handling 2020; Available from: https://www.worldcoal.com/handling/01052020/belt-conveyor-danger-zones/#:~:text=In%20most%20applications%2C%20a%20conveyor,(100%20%2D%202000%20fpm). .
27. *Engineering Toolbox*. 2001 2020; Available from: https://www.engineeringtoolbox.com.

Appendix A. Tabulated Motor/Drive System Performance Characterization Data

The dynamometer characterization results for the ZEUS radial flux surface permanent magnet AC motor and Allen Bradley VFD are provided in Table 16. The uncertainty in each direct measurement is equivalent to the accuracies specified in Table 6. Efficiency was calculated from the ratio of shaft output power (the product of torque and speed) to the electrical input power. This generated a propagated uncertainty of ±0.249% in efficiency. Efficiencies were unable to be measured at 25%–75% load setpoints at 300 RPM, so those efficiencies were interpolated to a curve fit to the other data points.

Table 16. ZEUS 15 HP RF-sPMAC and Allen Bradley VFD Dynamometer Characterization Results

(10 Hz, 25%–75% load results fit to curve of other data points)

	Target Point	Speed (RPM)	Torque (N-m)	Power Out (kW)	System Efficiency (%)	Power In (kW)
60Hz	110% Load	1,800	64.9	12.23	92.3%	13.25
	100% Load	1,800	59	11.12	92.0%	12.09
	90% Load	1,800	53.1	10.00	91.9%	10.89
	75% Load	1,800	44.25	8.34	92.3%	9.03
	50% Load	1,800	29.5	5.56	89.1%	6.24
	25% Load	1,800	14.75	2.78	89.2%	3.12
46.7Hz	110% Load	1,400	64.9	9.51	91.3%	10.42
	100% Load	1,400	59	8.65	90.8%	9.52
	90% Load	1,400	53.1	7.78	90.7%	8.58
	75% Load	1,400	44.25	6.48	91.1%	7.12
	50% Load	1,400	29.5	4.32	87.9%	4.92
	25% Load	1,400	14.75	2.16	87.6%	2.47
33.3Hz	110% Load	1,000	64.9	6.79	89.9%	7.55
	100% Load	1,000	59	6.18	89.8%	6.87
	90% Load	1,000	53.1	5.56	89.8%	6.19
	75% Load	1,000	44.25	4.63	90.1%	5.14
	50% Load	1,000	29.5	3.09	86.6%	3.56
	25% Load	1,000	14.75	1.54	85.5%	1.81
20Hz	110% Load	600	64.9	4.08	86.1%	4.73
	100% Load	600	59	3.71	85.1%	4.35
	90% Load	600	53.1	3.33	84.6%	3.94
	75% Load	600	44.25	2.78	84.4%	3.29
	50% Load	600	29.5	1.85	81.6%	2.27
	25% Load	600	14.75	0.93	80.6%	1.15
10Hz	110% Load	300	64.9	2.04	79.1%	2.58
	100% Load	300	59	1.85	78.4%	2.36
	90% Load	300	53.1	1.67	77.5%	2.15

	Target Point	Speed (RPM)	Torque (N-m)	Power Out (kW)	System Efficiency (%)	Power In (kW)
	75% Load	300	44.25	1.39	77.0%	1.81
	50% Load	300	29.5	0.93	73.6%	1.26
	25% Load	300	14.75	0.46	62.7%	0.74